Journal of Controlled Release 354 (2023) 323–336

Contents lists available at ScienceDirect

Journal of Controlled Release

journal homepage: www.elsevier.com/locate/jconrel

Tailoring surface properties of liposomes for dexamethasone intraocular administration

M.D. Al-Amin [a], Francesca Mastrotto [a], Astrid Subrizi [b,c], Merve Sen [d], Tiina Turunen [c], Blanca Arango-Gonzalez [d], Marius Ueffing [d], Alessio Malfanti [e], Arto Urtti [b,c], Stefano Salmaso [a,*], Paolo Caliceti [a]

[a] Department of Pharmaceutical and Pharmacological Sciences, University of Padova, Via F. Marzolo 5, Padova 35131, Italy
[b] School of Pharmacy, Faculty of Health Sciences, University of Eastern Finland, Yliopistonranta 1 B, Mediteknia Building, Kuopio, Finland
[c] Faculty of Pharmacy, University of Helsinki, Viikinkaari 5 E, Helsinki, Finland
[d] Centre for Ophthalmology, Institute for Ophthalmic Research, University of Tübingen, Elfriede-Aulhorn-Str. 7, Tübingen D-72076, Germany
[e] Advanced Drug Delivery and Biomaterials, Louvain Drug Research Institute, UCLouvain, Brussels 1200, Belgium

ARTICLE INFO

Keywords:
Liposome surface engineering
Retinal drug delivery
Cell penetration enhancers
Vitreal diffusion

ABSTRACT

Diseases of the posterior eye segment are often characterized by intraocular inflammation, which causes, in the long term, severe impairment of eye functions and, ultimately, vision loss. Aimed at enhancing the delivery of anti-inflammatory drugs to the posterior eye segment upon intravitreal administration, we developed liposomes with an engineered surface to control their diffusivity in the vitreous and retina association. Hydrogenated soybean phosphatidylcholine (HSPC)/cholesterol liposomes were coated with (agmatinyl)$_6$-maltotriosyl-acetamido-N-(octadec-9-en-1-yl)hexanamide (Agm$_6$-M-Oleate), a synthetic non-peptidic cell penetration enhancer (CPE), and/or 5% of mPEG$_{2kDa}$-DSPE. The zeta potential of liposomes increased, and the mobility in bovine vitreous and colloidal stability decreased with the Agm$_6$-M-Oleate coating concentration. Oppositely, mPEG$_{2kDa}$-DSPE decreased the zeta potential of liposomes and restored both the diffusivity and the stability in vitreous. Liposomes with 5 mol% Agm$_6$-M-Oleate coating were well tolerated by ARPE-19 retina cells either with or without mPEG$_{2kDa}$-DSPE, while 10 mol% Agm$_6$-M-Oleate showed cytotoxicity. Agm$_6$-M-Oleate promoted the association of liposomes to ARPE-19 cells with respect to plain liposomes, while mPEG$_{2kDa}$-DSPE slightly reduced the cell interaction. Dexamethasone hemisuccinate (DH) was remotely loaded into liposomes with a loading capacity of ~10 wt/wt%. Interestingly, mPEG$_{2kDa}$-DSPE coating reduced the rate of DH release and enhanced the disposition of Agm$_6$-M-Oleate coated liposomes in the ARPE-19 cell cytosol resulting in a more efficient anti-inflammatory effect. Finally, mPEG$_{2kDa}$-DSPE enhanced the association of DH-loaded Agm$_6$-M-Oleate coated liposomes to explanted rat retina, which reflected in higher viability of inner and outer nuclear layer cells.

1. Introduction

Ocular diseases such as age-related macular degeneration (AMD), glaucoma, and diabetic retinopathies are among the major causes of visual impairment and blindness. It has been predicted that the number of patients suffering from retinal diseases will increase globally by about 45% in the next 20 years due to the aging population [1].

Diseases of the posterior eye segment are characterized by increased retina inflammation mediated by secretion of IL-1, IL-6, IL-8, tumor necrosis factor (TNF-α), and granulocyte-macrophage colony-stimulating factor (GMC-SF) [2]. Furthermore, dysregulation of various growth factors, including vascular endothelial growth factors (VEGF), leads to pathological neovascularization with irreversible vision impairment [3].

Although several anti-VEGF and anti-inflammatory agents are commonly used to treat ocular diseases of the posterior segment, the biological barriers strongly limit their therapeutic performance. Indeed, the inner and outer blood-retinal barrier, blood-aqueous barrier, and corneal barrier limit the biodistribution of drugs either from systemic circulation or from the ocular surface after topical application [4]. Therefore, to overcome the low accessibility of drugs to the target tissues, most drugs to treat retinal diseases are administered *via* intravitreal

* Corresponding author.
E-mail address: stefano.salmaso@unipd.it (S. Salmaso).

https://doi.org/10.1016/j.jconrel.2023.01.027
Received 12 September 2022; Received in revised form 31 December 2022; Accepted 9 January 2023
Available online 16 January 2023

injections. However, while small molecules may permeate across the retina layers, they suffer from rapid drug clearance, thus requiring frequent injections, which entails the risk of severe adverse effects and infections. On the other hand, macromolecules and nanomedicines suffer from low retinal permeation, thus requiring delivery improvements to achieve therapeutic benefit [5,6].

Nanomedicine is expected to contribute to fulfilling the unmet needs of intraocular disease treatment with innovative approaches that provide sustained drug delivery to the posterior eye segment while reducing the frequency of administration. Accordingly, novel drug delivery systems have been explored to improve the bioavailability and biodistribution of therapeutic agents in the eye [7], enhance barrier penetration [8], exploit active targeting [9] or control the release profile of drug payload [10].

Liposomes are promising carriers that can be properly designed for controlled release and extended half-life of drugs in the vitreous [11]. Although the only liposome-based nanomedicine approved for AMD treatment, named Visudyne®, is administered intravenously, there is a growing interest in developing novel liposomal formulations for intravitreal administration of corticosteroids, antibiotics, chemotherapeutic, peptides or oligonucleotides [12–14]. Liposomes can, in fact, be decorated with functional components such as polymers, targeting agents, and cell penetration enhancers (CPEs), to tailor their biopharmaceutical feature and selectively trigger the drug release, tune the access across biological barriers, and modulate the intravitreal mobility to prolong the residence time or facilitate cell retina targeting [15–18].

Here, we report a liposomal system with tailored surface properties for intravitreal administration of anti-inflammatory drugs to the posterior eye segment. We explored the liposome decoration with a synthetic CPE and mPEG. CPE was used to promote the liposome association and uptake to the retina. Indeed, its cationic charge may slow the liposome diffusion through the vitreous due to electrostatic interactions with its components. The biopharmaceutical properties of the CPE-coated liposomes can be further modulated by PEG addition to the coating layer.

The liposomes of this study are expected to offer some benefits over Ozurdex, the intravitreal implant for dexamethasone release [19], although final clinical performance has not yet been shown. Firstly, they can be injected with a small needle (30 G) like chronic anti-VEGF medications and unlike Ozurdex (22 G). Secondly, Ozurdex is dislocated from vitreous body into the anterior chamber at incidence of 0.63% - a rare but serious complication that requires immediate action to avoid corneal edema [20]. Liposomes are eliminated from the vitreous anteriorly, but they are so small that they are eliminated from the anterior chamber in the aqueous humor outflow [21]. Thirdly, the lens opacification is a common side-effect of corticosteroids, like dexamethasone [22]. As liposomes permeate to retina, but not to the lens, liposomal dexamethasone might have beneficial therapeutic index compared to the suspensions and Ozurdex. Also, dexamethasone hemisuccinate, used in this study, may have lower permeation to the lens tissue than dexamethasone. Future comparative studies should inform whether liposomal dexamethasone will have improved therapeutic index over clinical state-of-art.

2. Materials and methods

2.1. Materials

Hydrogenated soybean phosphatidylcholine (HSPC, ≥98%, Tm 52.5 °C) was obtained from Lipoid GmbH (Ludwigshafen, Germany). Cholesterol was purchased from Sigma-Aldrich (St Louis, MO-USA). Dexamethasone hemisuccinate (DH, 1,4-pregnadien-9α-fluoro-16α-methyl-11β, 17, 21-triol-3, 20-dione 21-hemisuccinate) was purchased from Steraloids Inc. (Newport, R.I., USA). 1,2-distearoyl-sn-glycero-3-phosphoethanolamine-N-[methoxy(polyethylene glycol)-2000] [mPEG $_{2kDa}$-DSPE] and 1,2-dioleoyl-sn-glycero-3-phospho-(1′-rac-glycerol) (sodium salt) [DOPG] were purchased from Avanti Polar Lipids (Alabaster, Alabama, USA). N-(lissamine rhodamine B sulfonyl)-1,2-dihexadecanoyl-sn-glycero-3-phosphoethanolamine triethylammonium salt (rhodamine-DHPE) and N-(fluorescein-5-thiocarbamoyl)-1,2-dihexadecanoyl-sn-glycero-3-phosphoethanolamine triethylammonium salt (Fluorescein-DHPE) were obtained from VWR International PBI (Radnor, PA, USA). All buffer salts, solvents, and other reagents were purchased from VWR International PBI (Radnor, PA, USA) and Sigma-Aldrich (St. Louis, MO, USA).

Fetal bovine serum (FBS), L-glutamine (200 mM), sterile Dulbecco's phosphate-buffered saline (PBS), penicillin-streptomycin solution (10,000 units penicillin and 10 mg streptomycin/mL), L-glutamine (200 mM), trypsin (10×), lipopolysaccharides from *Escherichia coli* O111:B4 (LPS), 3-(4,5-dimethylthiazol-2-yl)-2,5-diphenyltetrazolium bromide (MTT) were purchased from Sigma-Aldrich (St. Louis, MO, USA). Dulbecco's modified eagle medium/nutrient mixture F-12 without glutamine was purchased from Aurogene (Rome, Italy). TrypLE™ Express, Gibco™ DMEM-F12 cell culture medium, and wheat germ agglutinin-Alexa Fluor 633 conjugates (WGA-Alexa Fluor633) were obtained from Thermo Fisher Scientific (Madison, WI, USA). Paraformaldehyde (PFA) was purchased from Polysciences Inc. (Warrington, PA, USA). IL-6 ELISA development kit was acquired from Mabtech AB (Nacka Strand, Sweden). *In-situ* cell detection kit was purchased from Roche applied science (Penzberg, Germany). Tissue-TEK®OCT™ was acquired from Sciences Services GmbH (Munich, Germany). 4′,6-diamidino-2-phenylindole (DAPI) was purchased from Vector laboratories Inc. (Burlingame, CA, United States).

2.2. Synthesis of (agmatinyl)$_6$-maltotriosyl-acetamido-N-(octadec-9-en-1-yl)hexanamide [Agm$_6$-M-Oleate]

The synthesis of (agmatinyl)$_6$-maltotriosyl-*N*-acetyl-amino-hexanoic acid (Agm$_6$-M-COOH) was performed as previously reported [23]. Agm$_6$-M-COOH (500 mg, 0.188 mmol) was dissolved in 5 mL of anhydrous dimethylsulfoxide (DMSO) and added 2.5 mL of 155.2 mg/mL N, N′-dicyclohexylcarbodiimide (DCC; 1.88 mmol) anhydrous DMSO solution. The reaction mixture was stirred for 15 min, and then added of 216.4 mg of N-hydroxysuccinimide (NHS; 1.88 mmol). After overnight stirring, the dicyclohexylurea was removed from the reaction mixture by filtration, and the solution of NHS-activated Agm$_6$-M-COOH was added of 619 μL of oleylamine (1.88 mmol) and 262 μL of triethylamine (1.88 mmol). The final mixture was stirred for 24 h and dropwise added to 500 mL of diethyl ether. The precipitate was desiccated, dissolved in water, and then lyophilized (93.6% molar yield). The product was characterized by ^{1}H NMR, and the guanidium content was assessed by Sakaguchi assay [24] according to a calibration line obtained with agmatine (y = 0.0663×-0.0183, R^2 = 0.9933).

^{1}H NMR (400 MHz, DMSO-d_6): δ 7.94–7.43 (m, 24H, guanidinium moieties), 5.32 (s, 2H, -C*H*=C*H*-), 3.10 (s, 12H, -CH_2-N-), 1.97 (bs, 4H, CH_2-C=C-CH_2) 1.23 (s, 36H, (CH_3)$_2$-C-), 0.85 (s, 3H, -CH_3).

2.3. Liposome formulation

Liposomes were prepared by thin layer hydration technique [25]. Briefly, 20 mg mixtures of 2:1 HSPC/cholesterol molar ratio for neutral naked liposomes (*Naked Lipo*) or 2:1:1 of HSPC/ DOPG/Cholesterol molar ratio for anionic liposomes (*Anionic Lipo*) were prepared from 6.7 mg/mL stock chloroform solutions of each lipid. Rhodamine-DHPE or fluorescein-DHPE (0.3 mol% of with respect to lipids) were included in the lipid mixture to generate fluorescently labeled liposomes. The solutions were transferred to a round bottom flask, and the organic solvent was removed under reduced pressure using a rotary evaporator. The lipid film was then hydrated using 1 mL of 10 mM HEPES, 150 mM NaCl, pH 7.4 (HEPES buffer). The samples were processed with 10 freeze-thaw cycles and extruded 11 times using a 200 nm cut-off polycarbonate membrane mounted in Avanti mini extruder (Avanti Polar Lipids Inc. Alabaster, Alabama, USA) and diluted to a final lipid concentration of

10 mg/mL.

2.4. Liposome coating

Neutral naked liposomes, $mPEG_{2kDa}$-DSPE, Agm_6-M-Oleate solutions, and HEPES buffer were preincubated 5 min at 45 °C. Neutral naked liposomes were mixed with fixed volumes of 6 mg/mL $mPEG_{2kDa}$-DSPE (mPEG) and/or 4 mg/mL Agm_6-M-oleate (CPE) solutions in HEPES buffer. The mixtures were diluted to a final lipid concentration of 2.5 mg/mL with the same buffer, followed by incubation at 45 °C for 10 min in an Eppendorf Thermomixer F 2.0 (Hamburg, Germany). Decorated liposomes with the following compositions were obtained: (i) 5 mol% $mPEG_{2kDa}$-DSPE liposomes (*PEG-Lipo*); (ii) 5 mol% Agm_6-M-oleate liposomes (*Agm_6-Lipo*); (iii) 5 mol% of Agm_6-M-oleate and 5 mol % of $mPEG_{2kDa}$-DSPE liposomes (m*PEG/5%Agm_6-Lipo*); (iv) 10 mol% of Agm_6-M-oleate liposomes (*10%Agm_6-Lipo*) (v) 10 mol% of Agm_6-M-oleate and 5 mol% of $mPEG_{2kDa}$-DSPE liposomes (*mPEG/10%Agm_6-Lipo*). The percentages of functional components are referred to the lipids in the formulations. Preliminary studies were performed by decorating liposomes at increasing Agm_6-M-oleate ratio in the 0–20 mol % range.

The amount of Agm_6-M-oleate associated to the liposomal bilayer was tested by liposome centrifugation for 20 min at 15,000 rpm (Sigma 1–14 microfuge, Newtown, UK) and assessing the guanidinium group and lipid concentrations in the supernatant by Sakaguchi assay and Stewart assay ($y = 8.932\times + 0.0079$, $R^2 = 0.99$), respectively [24,26,27].

The amount of $mPEG_{2kDa}$-DSPE associated to liposomes was tested on the pellet by Iodine assay [28], *and the percentage of* $mPEG_{2kDa}$-DSPE inserted was calculated with *respect to lipids in the pellet assessed by* Stewart assay [27].

2.5. Dexamethasone hemisuccinate loaded liposomes

Dexamethasone hemisuccinate (DH)-loaded liposomes were formulated according to the remote loading technique reported in the literature [29]. Naked liposomes were prepared by lipid film hydration with 1 mL of 0.2 M calcium acetate, and calcium acetate-loaded liposomes were dialyzed overnight using a 100 kDa float-a-lyzer against 1 L of HEPES buffer to remove the non-loaded calcium acetate. The resulting lipid concentration after dialysis was assessed by the Stewart assay [27]. A 5 mg/mL DH stock solution in HEPES buffer was added to the liposomes to yield 10 mg/ mL lipids and 2.5 mg/mL DH mixture that were incubated at 65 °C for 60 min. The non-loaded DH was removed by 12 h dialysis using a 100 kDa float-a-lyzer against HEPES buffer.

DH-loaded liposomes were surface modified with 5 mol% Agm_6-M-oleate, or with 5 mol% $mPEG_{2KDa}$-DSPE, or 5 mol% Agm_6-M-oleate/ $mPEG_{2KDa}$-DSPE according to the post-insertion procedure reported above. DH leaked during the coating, and the non-associated Agm_6-M-oleate were removed by liposome centrifugation at 15,000 rpm for 20 min at 4 °C (Beckman L780, Indianapolis, IN, United States). The centrifuged liposomes were re-dispersed in the same buffer at the concentrations requested for further studies.

Loading of DH into the liposomes was assessed by spectrophotometric analysis. Twenty μL of liposomes were dispersed in 800 μL of methanol and sonicated for 30 min to induce lipid dissociation and analyzed by UV–Vis at 242 nm. All experiments were performed in triplicate.

Loading capacity and loading efficiency were derived using the following equations:

$$\text{Loading capacity } (w/\text{w}\%) = \frac{DH\ encapsulated\ (mg/mL)}{Lipids\ (mg/mL)} \text{ x } 100 \quad (1)$$

$$\text{Loading efficiency } (\%) = \frac{DH\ encapsulated\ (mg/mL)}{fed\ DH\ (mg/mL)} \text{ x } 100 \quad (2)$$

2.6. Size and zeta potential analyses

Size, poly-dispersity index (PDI), and zeta potential of liposomal formulations were measured by photo correlation spectroscopy (PCS) using a Malvern Zetasizer NanoZS (Malvern, UK). Size and poly-dispersity index (PDI) were analyzed using liposomes diluted to 0.2 mg/mL in HEPES buffer or cell culture media (DMEM-F12, Gibco™) or homogenized vitreous. Zeta potential was assessed by using liposomes diluted to 0.2 mg/mL in mQ water.

2.7. Cryogenic electron microscopy (Cryo-EM)

Three μL of liposomes at 2.5 mg/mL lipid concentration were vitrified with Leica EMGP vitrification device (Leica Microsystems GmbH, Wetzlar, Germany) using freshly glow discharged Quantifoil Cu R1.2/ 1.3 grids. Images of the vitrified samples were acquired with FEI TALOS Artica transmission electron microscope (Cryo-EM unit, University of Helsinki) equipped with Falcon III direct electron detector camera and FEI phase plate at 57000× magnification.

2.8. Colloidal stability

Samples of 2.5 mg/mL DH-loaded liposomal formulations in HEPES buffer, were incubated at 37 °C. At scheduled time points, the samples were diluted to 0.2 mg/mL, and size, PDI, and zeta potential were assessed by PCS as reported above.

The colloidal stability of liposomal formulations was also tested in porcine vitreous. The vitreous was mechanically homogenized with a 40 mL Dounce tissue grinder (Wheaton™, Thermo Fisher Scientific, Madison, WI, USA), followed by centrifugation at 3600 *g* for 1 h. The homogenate was sequentially filtered twice with a sterile 0.45 μm filter and twice with sterile 0.22 μm filter and stored at −80 °C until use. 0.3 mol% fluorescein-DHPE labeled liposomes at 2.5 mg/mL in HEPES buffer were mixed with homogenized vitreous in a 1:1 *v*/v ratio. Flow cytometry (Apogee Flow Systems, Hertfordshire, UK) was used to differentiate between the liposomes and porcine macromolecular vitreous components by large-angle light scattering (LALS), and the detection of the fluorescein-DHPE fluorescence was used to identify the liposome population. Large angle light scattering (LALS) of each formulation was measured at day 0 and day 20.

2.9. Diffusivity in vitreous

Freshly explanted porcine eyeballs provided by the slaughterhouse HKScan (Forssa, Finland) were treated to remove the extraocular tissue and washed with PBS. The eye preparation was performed following the protocol in the literature [30,31]. Briefly, the eyeballs were placed on Petri dishes, and the anterior ocular parts were cut and removed by performing a short incision into the sclera perpendicularly to the anterior-posterior axis using a scalpel blade. Then, after the removal of the anterior eye section, the intact vitreous body was left in the posterior part of the eye (Fig. SI-1). Afterwards, the intravitreal injection of liposomal formulations was performed using a 30G BD Micro-Fine™ insulin syringe (BD, Franklin Lakes, USA). The liposome samples were injected at a depth of 0.5 cm inside the vitreous. The injections contained 50 μL of 0.5, 0.1, and 0.01 mg/mL of 0.3 mol% rhodamine-DHPE labeled liposomal formulations in HEPES buffer. The eye samples were covered with 35 mm microwell dishes having 14 mm diameter glass window at the bottom (MatTek Corporation, Ashland, MA, USA). Thereafter, the eyeballs were inverted upside down, leaving the vitreous facing down and the posterior eyeball facing up, and fixed using Loctite Precision® super glue before performing the confocal analysis at 37 °C. Each liposome formulation was tested with at least three different porcine eyes. Ten videos were recorded, and four of them were processed to derive the values of mean square displacement (MSD) and the

diffusion coefficient.

Rhodamine-DHPE labeled liposomes were tracked using a 3I Marianas confocal microscope equipped with an Andor Neo sCMOS camera using the 561 nm laser source. Slidebook® 6 software (Intelligent Imaging Innovation, Colorado, USA) was used to record 15 s movies at 150 ms temporal resolution. The movements of liposomes in the intact vitreous were analyzed using Imaris software (Bitplane AG, Zurich, Switzerland) with MATLAB plug-in (The MathWorks, Inc. Massachusetts, USA). The obtained MSD values were used to determine the diffusion coefficient in vitreous (Dv) using equation Eq. (3). As controls, the diffusion coefficient in water was theoretically calculated considering liposome size obtained by PCS analysis (Eq. (4))

$$Dv = \frac{MSD}{4t} \tag{3}$$

$$Dw = \frac{RT}{6\pi\eta rN} \tag{4}$$

where *MSD* is the mean-squared displacement of liposome trajectories, *t* is the time delay for the calculated displacement, *R* is the gas constant (8.314 J K^{-1} mol^{-1}), *T* is the temperature (310.15 K), η is the viscosity of vitreous at 37 °C, *r* is the size of liposomes obtained from PCS measurements, and *N* is the Avogadro constant (6.022 × 10^{23} mol^{-1}).

2.10. Drug release

The release of DH from liposomes was evaluated *in vitro*. A dispersion of 1 mL of 2.5 mg/mL DH-loaded liposomes in HEPES buffer was transferred into a 20 KDa MWCO Spectra/Por® Float-A Lyzer® and dialyzed against 4 L of the same buffer. The dialysis system was maintained at 37 °C. At scheduled times, 10 μL of liposome suspension was withdrawn from the dialysis bag and diluted with 500 μL methanol to assess the DH concentration by UV-spectrophotometry. The release study was carried out for 30 days.

2.11. Cell culture

ARPE-19 (ATCC® CRL-2302), retinal pigment epithelial cells, were cultured at 37 °C in a 5% CO_2 atmosphere using DMEM-F12 medium (Gibco™) supplemented with 10% FBS, 2 mM L-Glutamine, 100 IU/mL penicillin and 100 μg/mL streptomycin. Cells at 70% confluency were subcultured by treatment with 0.05% trypsin-0.02% EDTA solution (Sigma-Aldrich, St. Louis, MO, USA).

2.12. Cytotoxicity studies

In vitro cytotoxicity of DH-loaded liposomes was performed with human retinal pigmented epithelial cell line (ARPE-19). ARPE-19 cells were seeded in a 96-well plate at a density of 3 × 10^4 cells/well and grown for 24 h in a humidified 5% CO_2 atmosphere at 37 °C using DMEM F-12 medium supplemented with 10% FBS, 2 mM L-glutamine, 100 IU/mL penicillin and 100 μg/mL streptomycin. Then the medium was discharged, and the cells were washed twice with PBS and incubated with 200 μL of DH-loaded liposomes or free DH in DMEM F12 without FBS at equivalent DH concentration of 1, 10, 20, 50, and 100 μM. Drug-free liposomes at equivalent lipid concentrations and higher, up to 1 mg/mL lipids, were tested. After 6 and 24 h, the medium was removed, and the cells were washed carefully with PBS and then incubated with 200 μL/well of complete medium added of 20 μL of 5 mg/mL MTT solution in PBS for three hours at 37 °C. The medium was removed, and 200 μL/well of DMSO was added. After 30 min, the plate was read spectrophotometrically with a microplate reader (Microplate autoreader, EL311SK, Biotek Inc., Vermont, USA) equipped with a 570 nm light filter. The analysis was done in triplicate, and cell viability was expressed as a percentage referring to non-treated cells.

2.13. Cell association

2.13.1. Cytofluorimetry

ARPE-19 cells (2 × 10^5 cells/well) were seeded on a 24-well plate in DMEM F12 supplemented with 10% FBS and grown for 24 h. The medium was discharged, and the cells were washed twice with PBS. Blanc liposomes or DH-loaded liposomes (volume 500 μL) with 0.3 mol% fluorescein-DHPE were added to each well in triplicate at concentrations of 0.1, 0.25, and 0.5 mg/mL. The cells were incubated with liposomes for 1 h. Afterwards, the liposome-containing medium was removed, and the cells were washed twice with PBS and once with PBS containing 10% FBS. Cells were then detached by treatment with 200 μL/well of 0.125 mg/mL trypsin for 8 min at 37 °C and then transferred in FACS tubes containing 200 μL PBS, 0.5 *w/v*% BSA, 5 mM EDTA, 2 mM NaN_3, 4 w/v % PFA. Cells were stored at 4 °C in the dark prior to analysis. Samples underwent cytofluorimetric analysis using a BD FACS CANTO™ II (BD Biosciences, San Jose, CA, USA), and fluorescence deriving from fluorescein-DHPE labeled liposomes was detected using a laser emitting at 496 nm.

2.13.2. Confocal microscopy

ARPE-19 cells (8 × 10^4/well) were seeded on 13 mm^2 cover slips introduced in a 24-well plate with DMEM F12 added of 10% FBS and grown for 24 h. The medium was then removed, and the cells were washed twice with PBS. 300 μL of a 0.1 mg/mL of DH-free and DH-loaded fluorescein-DHPE labeled liposomes in FBS free medium was added to each well, and cells were incubated for 1 h. Afterwards, the medium was removed, and the cells were washed twice with PBS and twice with PBS added of 10% FBS. Cells were then fixed by 20 min treatment with 200 μL/well PBS containing 4% (*w/v*) PFA. The solution was then discharged, and cells were washed three times with PBS. The staining of cell nuclei was performed by incubating the samples with 200 μL of a 5 μg/mL solution of DAPI in PBS for 10 min. After discharging the solution, cell membranes were stained by incubating cells with 200 μL/well of a 5 μg/mL solution of Wheat germ agglutinin-Alexa fluor-633 conjugate in PBS for 10 min. The solution was then discharged, and cells were washed with PBS three times and two times with mQ water. The coverslips were mounted on a glass slide using Mowiol as mounting medium. The samples were maintained at 4 °C in the dark until microscopic examination. Cell samples were imaged using a Zeiss LSM 800 confocal microscope (Carl Zeiss, Jena, Germany) equipped with a 63×, n.a. 1.4, oil immersion objective and a ZEN 2.1 - blue edition – software (Carl Zeiss, Jena, Germany). Lasers with emission wavelengths at 405, 488, and 640 nm were used to detect DAPI, fluorescein-DHPE, and WGA-Alexa Fluor-633, respectively. To avoid emission crosstalk, each emission fluorescence was recorded independently with specific detector and optical cut-off filter over the entire emission spectrum of related chromophores. Image analyses were performed using ImageJ 1.47v (National Institutes of Health software package).

2.14. In vitro anti-inflammatory assay

The anti-inflammatory activity of liposomes was investigated by quantifying the inhibition of pro-inflammatory cytokine release. 1.2 × 10^5 ARPE-19 cells/well were seeded in a 24-well plate using DMEM F12 medium and grown for 24 h in a humidified 5% CO_2 atmosphere at 37 °C. Then, the medium was discharged, and the cells were washed twice with PBS and incubated with 500 μL of 5 μg/mL LPS for 12 h. Afterwards, LPS was removed, and 500 μL of 1 and 10 μM DH-loaded liposomes, or DH solution at equivalent concentration or drug-free liposomes containing an equivalent concentration of lipids was added, and cells were incubated for 1 h. Media containing liposomes or free drug were removed, and cells were further incubated for 24 h in DMEM-F12 without FBS. Supernatants were collected after 24 h and analyzed with human IL-6 ELISA kit to quantify the IL-6 concentration in each group. Cells were lysed with 2% Triton X-100 in 10 mM Tris-HCl, 150

mM NaCl, 2 mM EDTA, pH 8.2, and cell number of each group was assessed by BCA assay. IL-6 concertation in the supernatants was normalized by cell number in each group.

In order to assess the carrier's pro-inflammatory activity, non-LPS stimulated cells were incubated with drug-free liposomes at lipid concentrations equivalent to those of the 1 and 10 μM DH-loaded liposomes for 12 h. Afterwards, liposomes containing medium was removed, cells were washed with PBS and further incubated with medium without FBS for 24 h. Cell supernatants were then tested as reported above.

2.15. Distribution and therapeutic activity in ex-vivo retinal organ culture

Penetration and neuroprotective effects of DH-loaded liposomes were evaluated in *ex-vivo* retinal organ culture. All procedures were approved by the Tübingen University committee on animal protection and performed in compliance with the Association for Research in Vision and Ophthalmology (ARVO) statement. Animals were kept in the Tübingen Institute for Ophthalmic Research animal housing facility under standard white cyclic lighting, had free access to food and water, and were used irrespective of sex unless stated otherwise. All efforts were made to minimize the number of animals used and their suffering.

Retinal explants were cultured as previously described [32–34]. Briefly, 6 days-old WT C57BL/6 J mice were sacrificed, and the eyes were removed and incubated for 15 min at 37 °C in a 12% Proteinase K solution. First, enzymatic digestion was quenched by transferring the eyes to HBSS medium, added of 10% fetal bovine serum, and incubating them for 5 min at room temperature. Next, the eyes were dissected in HBSS medium: (1) the sclera was carefully removed, leaving the retinal pigmented epithelium attached to the eyeball; (2) the incisions were made at the edge of the cornea to remove the cornea, lens, and hyaloid body; (3) four equidistant, radial incisions were made in the retina.

The retinas were then transferred, with retinal pigmented epithelium side down, to a nitrocellulose culture membrane (PICMORG50, Millipore) and cultured in Neurobasal A medium (NA, Gibco, Carlsbad, CA, USA) supplemented with 2% B-27 supplement (Gibco, Carlsbad, CA, USA), 1% N2 supplement (Invitrogen, Carlsbad, CA, USA), 1% penicillin solution (Gibco, Carlsbad, CA, USA), and 0.4% GlutaMax (Gibco, Carlsbad, CA, USA). Explants were maintained for 5 days at 37 °C in a humidified 5% CO_2 atmosphere. To mimic dosing *via* intravitreal treatment (IVT), treatments were given apically as 15 μL drops containing 135 μg/mL of free DH and DH equivalent DH-loaded liposomes. Untreated neurobasal medium was used as control. Explants were incubated with treatments for 5 days.

After treatment, retinal explants were fixed in 4% PFA (Polysciences, Inc., Warrington, PA, USA) at room temperature for 40 min. Retinas were then washed with PBS for 20 min and cryoprotected by incubation with 10, 20, and 30% sucrose solution for 20 min each. After that, tissues were embedded in Tissue-TEK® OCT™ (Science Service, GmbH, Munich, Germany), and sections were frozen in liquid nitrogen. Next, 14 μm vertical sections were obtained on an HM525 NX Cryostat (Thermo Fisher GmbH, Dreieich, Germany), air-dried at 37 °C for 1 h, and stored at −20 °C until use.

In situ cell death detection kit by Roche Applied Sciences (Penzberg, Germany) was used according to the supplier's protocol. The apoptotic nuclei count was expressed as the ratios of TUNEL-positive nuclei over DAPI-stained nuclei for each of the three nuclear layers in the sections of the same group.

All samples underwent microscopic imaging using Zeiss Axio Imager Z1 ApoTome microscope, AxioCam MRm camera, and Zeiss Zen 2.3 software in *Z*-stack at 20 × magnification. For quantitative analysis, positive cells in the outer nuclear layer (ONL) and inner nuclear layer (INL) of at least three sections per group were counted. The percentage of positive cells was derived from the number of positive cells by the total number of cells in each layer. In addition, photoreceptor cell rows were assessed by counting the individual nuclei rows in one ONL and INL and averaging the counts.

2.16. Statistical analysis

The results of the experiments were expressed as mean ± SD derived from three independent experiments. The significance of the difference between treatment groups was determined by the two-tailed Student's *t*-test using GraphPad Prism 5 software (La Jolla, CA, USA).

3. Results and discussion

To achieve retinal delivery and sustained release of anti-inflammatory drugs, dexamethasone hemisuccinate (DH)-loaded liposomes with tailored intravitreal diffusion and cell up-take were designed. DH was used in place of dexamethasone because this prodrug can be efficiently loaded into liposomes by remote loading [29,35]. Dexamethasone is largely used as an anti-inflammatory drug for AMD treatment [19], and the hemisuccinate prodrug was found to display the anti-inflammatory activity of the native drug [36].

Liposomes were decorated with oligocationic moieties because cationic liposomes have been found to efficiently deliver drugs to retinal cells [37–39]. Furthermore, the oligicationic functions used to decorate liposomes were shown to enhance the cellular uptake of colloidal systems [40]. Cationic liposomes interact electrostatically with the negatively charged macromolecular components of the vitreous (*i.e.*, hyaluronic acid), slowing the elimination from the vitreal cavity [16]. Monomethoxy-poly(ethylene glycol) (mPEG) was added to modulate the mobility of liposomes in the vitreous. PEG has been reported to enhance the mobility of nanocarriers, such as cationic liposomes, in viscous physiologic matrices, such as vitreous and respiratory mucous [41] or female reproductive tract mucous [42–44]. Furthermore, PEG can modulate the cell interaction of cationic liposomes lowering cytotoxicity typical of cationic nanoparticles and thus enhancing biocompatibility [45,46].

3.1. Liposome composition study

The oligocationic moiety used for liposome decoration was obtained by end-tipping oleylamine with an oligo-agmatine maltotriosyl-*N*-acetyl-amino-hexanoic acid derivative (Agm_6-M-COOH). The Agm_6-M-CO-X-R derivatives were previously found to be excellent carriers for nucleic acids [23,47] and cell permeation enhancers upon conjugation to proteins or liposomes [40,48].

The oleyl function of oligocationic "star-like" Agm_6-M-oleate (Scheme 1) was introduced for lipid anchoring to the liposomal bilayer. The ^{1}H NMR analyses confirmed the chemical identity of the synthesized Agm_6-M-oleate. Indeed, the 2 protons integration of the signal at 5.32 ppm of the Z-hydrogens on the -C=C- double bond and the 3 protons integration of the signal at 0.85 ppm of the terminal methyl group of the oleyl moiety are in agreement with the expected 36 proton integration of the signal at 1.23 ppm of the hydrogens of the methyl groups of the isobutyryl moieties.

Liposome decoration was achieved by post-insertion of Agm_6-M-oleate and mPEG-DSPE.

Fig. SI-2A shows the efficiency of Agm_6-M-oleate insertion to the liposomes: theoretical 10 mol% Agm_6-M-oleate feeding yielded more than 96% association of oligocationic moiety to the liposomes. At higher Agm_6-M-Oleate feeding ratios (>10 mol%), the association efficiency decreased. These results are in agreement with the zeta potential profile (Fig. 1A), showing that the zeta potential increases up to 32.7 ± 1.3 mV by Agm_6-M-oleate feeding but remains stable at Agm_6-M-oleate feeding ratios above 10 mol%. The size of liposomes was not affected by oligocationic moiety insertion (162–177 nm; Fig. SI-2B).

To investigate the effect of the positive charge density on liposome diffusion in the vitreous, liposomes with 5 and 10 mol% of Agm_6-M-oleate insertion were selected as formulations with medium (5%Agm_6-Lipo) and high (10%Agm_6-Lipo) positive charge densities, respectively.

PEGylated liposomes (mPEG-Lipo, mPEG/5%Agm_6-Lipo, mPEG/

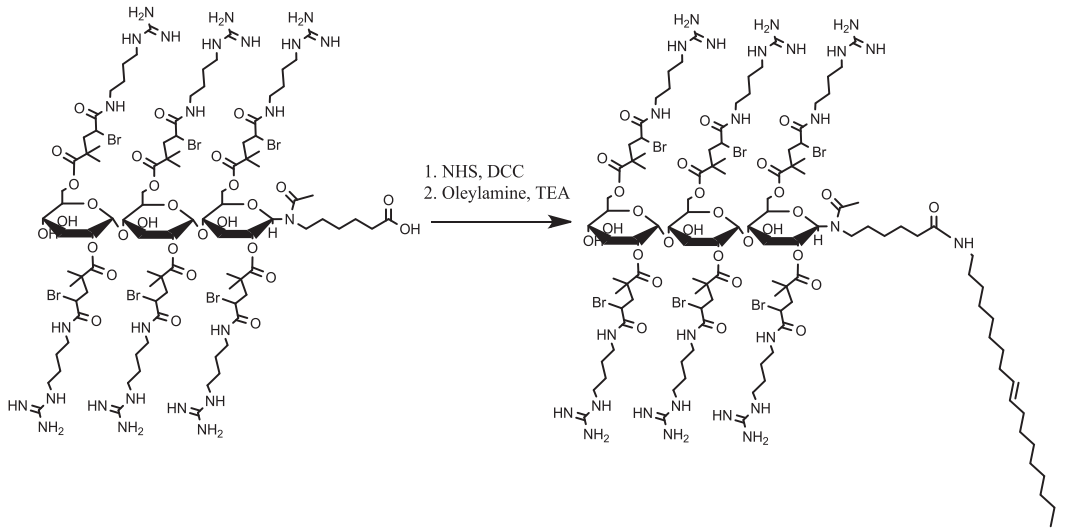

Scheme 1. Scheme of Agm_6-M-Oleate synthesis by conjugation of the Agm_6-M-COOH to oleylamine to yield (agmatinyl)$_6$-maltotriosyl-acetamido-N-(octadec-9-en-1-yl)hexanamide. Agm_6-M-COOH was synthesized according to Malfanti et al. [23].

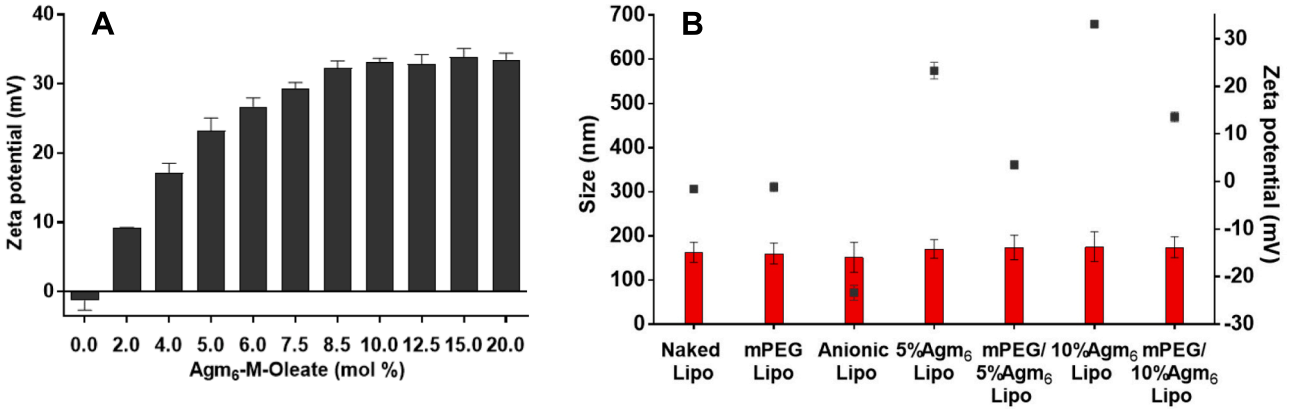

Fig. 1. Physical features of Agm_6-M-oleate and mPEG-DSPE coated liposomes. *A. zeta* potential of Agm_6-M-Oleate coated liposomes. B. Size (■) and zeta potential (■) of the liposome library: Naked-Lipo, PEG-Lipo, Anionic-Lipo, 5%Agm_6-Lipo, mPEG/5%Agm_6-Lipo, 10%Agm_6-Lipo, mPEG/10%Agm_6-Lipo.

10%Agm_6-Lipo) were obtained by post-insertion of 5 mol% $mPEG_{2kDa}$-DSPE, which is the mPEG content used in several pharmaceutical liposomal formulations [49]. According to the analysis of associated and non-associated mPEG-DSPE, the polymer association resulted to be 96%.

Neutral naked liposomes (*Naked-Lipo*, HSPC/Chol, 162.6 ± 22.6 nm, −1.3 ± 1.4 mV), neutral PEGylated liposomes (m*PEG-Lipo*, HSPC/Chol, 162.6 ± 22.6 nm, −1.1 ± 1.3 mV) and negatively charged liposomes (*Anionic-Lipo*, HSPC/DOPG/Chol, 151.4 ± 33.7 nm, −23.4 ± 1.5 mV)

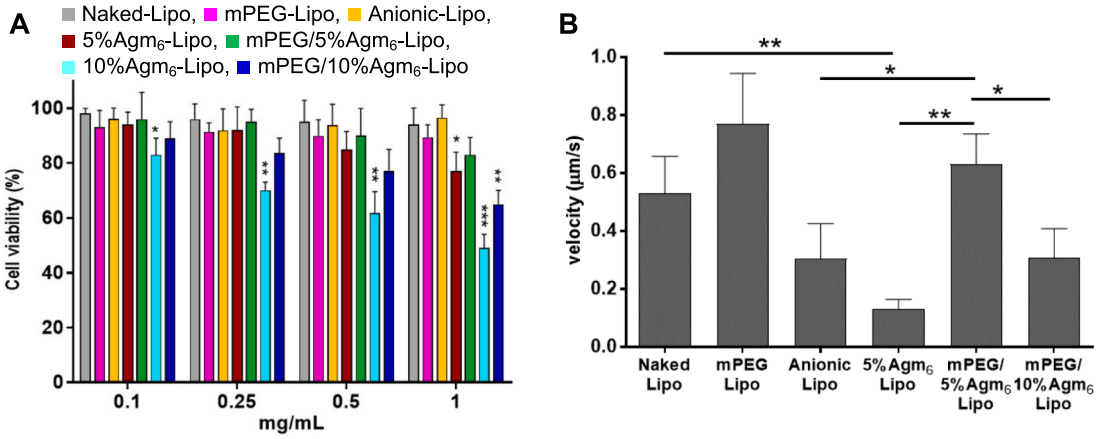

Fig. 2. A. Viability profile of ARPE-19 cells incubated for 6 h with liposomes at increasing lipid concentration. Statistical analysis *versus* Naked-Lipo: * $p < 0.05$, ** $p < 0.01$, *** $p < 0.001$. B. Mean velocity in vitreous of rhodamine-DHPE labeled liposomes. Statistical analysis: * $p < 0.05$, ** $p < 0.01$, *** $p < 0.001$.

were also prepared for comparative studies.

The results reported in Fig. 1B show that mPEG on the liposome surface does not affect either the size or the PDI of liposomes. On the contrary, mPEG reduced the zeta potential values of 5%Agm_6-Lipo and 10%Agm_6-Lipo by physical shielding of the cationic charges. The zeta potential reduction was higher for 5%Agm_6-Lipo (84.9%) than in 10% Agm_6-Lipo (58.9%), indicating that the masking effect of mPEG decreases as the cationic density increases.

3.2. Liposome behavior in the vitreous and cultured cells

3.2.1. Cytotoxicity

In-vitro results from cultured ARPE-19 cells reported in Fig. 2A show that Naked-Lipo, Anionic-Lipo, and mPEG-Lipo did not elicit cytotoxicity even at high liposome concentrations and 5%Agm_6-Lipo and mPEG/5%Agm_6-Lipo showed slight cytotoxicity only at high liposome concentration (1 mg/mL) The 10%Agm_6-Lipo displayed dose-dependent cytotoxicity. This is in agreement with the cytotoxicity of cationic nanoparticles that interact with negatively charged cell surface and may result in membrane disruption [50]. Interestingly, the charge shielding by mPEG reduced the cytotoxicity of the 10%Agm_6-Lipo. Due to the toxicity, 10%Agm_6-Lipo were not further investigated.

3.2.2. Vitreal diffusion

The mobility of liposomes in the vitreous affects their clearance and association with the retina [16]. Therefore, liposome mobility was investigated using *ex-vivo* porcine eye and rhodamine-DHPE-labeled liposomes.

Fig. SI-3 shows representative trajectories of liposomes imaged over time by confocal microscopy, and Fig. 2B reports the mean velocity (μm/s) obtained by tracking of at least 100 liposomes.

mPEG-Lipo were found to move faster (0.77 ± 0.13 μm/s) than Naked-Lipo (0.53 ± 0.11 μm/s) and Anionic-Lipo (0.30 ± 0.12 μm/s) (Fig. 2B). This is in agreement with the literature data reporting enhanced diffusion of PEG-coated liposomes in the vitreous [51]. 5% Agm_6-Lipo displayed the lowest mobility, presumably due to their positively charged surface that interacts with the negatively charged macromolecules in the vitreous (*e.g.*, hyaluronic acid) [51,52]. Addition of mPEG to the liposomes increased the mobility of 5%Agm_6-Lipo due to the masking of the positive charge on the liposome surface. In line with the zeta potential values, mPEG/10%Agm_6-Lipo showed lower vitreal mobility than mPEG/5%Agm_6-Lipo. Unexpectedly, Anionic-Lipo showed low mobility in the vitreous, which was similar to mPEG/10% Agm_6-Lipo (Fig. 3B). It is worth noting that the low mobility of anionic nanoparticles in the vitreous has already been reported in the literature [37], although another study reported high mobility of anionic liposomes in the vitreous [51]. This behavior may result from "wrong side interactions" that can be due to Coulombic and van der Waals interactions between the colloidal systems (*i.e.*, nanoparticles and macromolecules) occurring in complex matrices [53].

The diffusion coefficients in vitreous (D_v) and in water (D_w) are reported in Table 1; high D_w/D_v ratios indicate reduced particle mobility in the vitreous. The results suggest that the combination of mPEG-DSPE and Agm_6-M-oleate modulates the diffusivity of liposomes in physiological matrices. Importantly, mPEG increased the vitreal mobility of the cationic liposomes to the levels of neutral liposomes (Table 1).

3.2.3. Cell uptake

Cytofluorimetric and confocal analyses were performed with ARPE19 cells to study the cell association and uptake of fluorescein labeled liposomes. The results reported in Fig. 3-i show that the Naked-Lipo, Anionic-lipo, and mPEG-Lipo poorly associate with ARPE19 cells. On the contrary, positively charged liposomes remarkably associate with ARPE-19 cells; 5%Agm_6-Lipo yielded the highest cell association. Also, the PEGylated versions of Agm_6-coated liposomes showed high cell association, even though a few previous studies showed reduced liposome cell interaction after surface coating with PEG [54,55]. Apparently, PEG in mPEG/5%Agm_6-Lipo and mPEG/10%Agm_6-Lipo did not significantly interfere with the cell association, even though it prevented the liposomes from vitreal binding.

Table 1
Experimentally derived diffusion coefficients of liposomes in vitreous (D_v) and their theoretically calculated diffusion coefficients in water (D_w).

	D_v ($\mu m^2/s$)	D_w ($\mu m^2/s$)	D_w/D_v
Naked-Lipo	0.08282	2.70	32.60
mPEG-Lipo	0.17451	2.82	16.16
Anionic-Lipo	0.02786	3.00	107.68
5%Agm_6-Lipo	0.00408	2.65	649.51
mPEG/5%Agm_6-Lipo	0.10722	2.83	26.39
mPEG/10%Agm_6-Lipo	0.02090	2.82	134.93

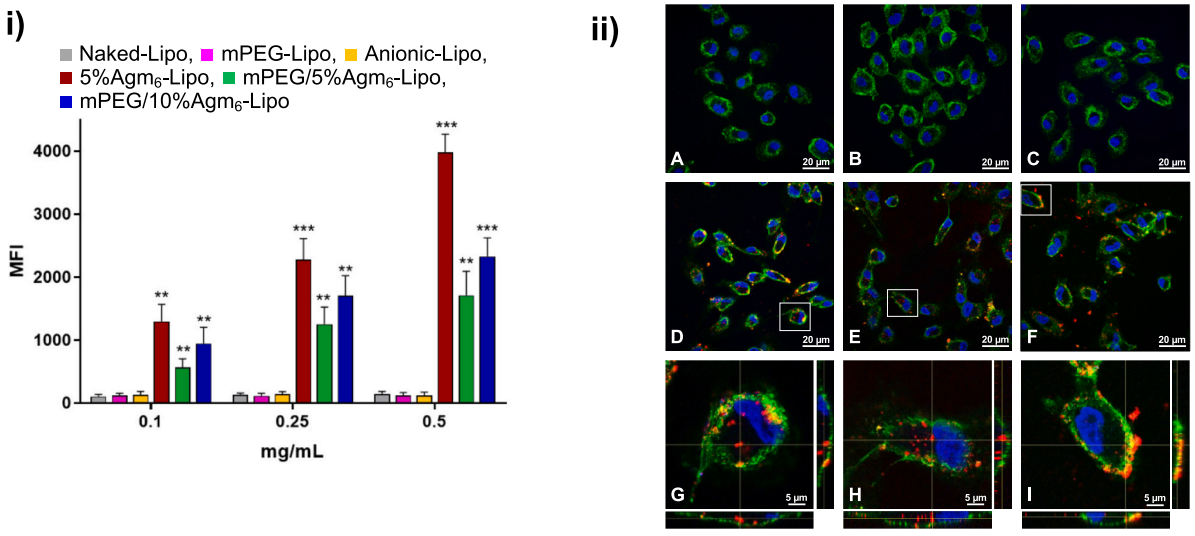

Fig. 3. i) Mean fluorescent intensity of ARPE-19 cells incubated with fluorescein-DHPE labeled pro-drug-free liposomes. Statistical analysis was calculated *versus* Naked-Liposomes. * $p < 0.05$, ** $p < 0.01$, *** $p < 0.001$, **** < 0.0001. ii) Confocal microscopic images of ARPE-19 cells incubated with pro-drug-free Naked-Lipo (A), mPEG-Lipo (B), Anionic-Lipo (C), 5%Agm_6-Lipo (D), mPEG/5%Agm_6-Lipo (E) and mPEG/10%Agm_6-Lipo (F). Magnification and *Z*-projection of the cells in the white squared areas of Panel D—F are reported in Panel G-I, respectively.

The confocal microscopy images reported in Fig. 3-ii confirmed the results of cell association studies. Incubation of Naked-Lipo, Anionic-Lipo, and mPEG-Lipo with ARPE-19 cells yielded negligible fluorescent spots in the cells (Fig. 3-ii A-C). On the contrary, remarkable cell uptake was observed with all cationic liposomes. In particular, 5%Agm_6-Lipo and mPEG/5%Agm_6-Lipo localized in the cytoplasm (Fig. 3-ii D-E), as confirmed by zeta stack projections of the magnified images (Fig. 3-ii G-H). Instead, mPEG/10%Agm_6-Lipo were mostly associated with the cell surface (Fig. 3-ii F and I). Overall, these results indicate that despite mPEG-induced zeta potential reduction, the interactions of cationic liposomes with cells were not prevented but affected their localization within cells. Indeed, other studies showed that the cationic charge / PEG ratio on the liposomal surface affects the association to and the uptake into cancer cells, and the cell membrane adhesion of liposomes increases over uptake when the ratio increases [56].

Based on cytofluorimetric and confocal results, Anionic-Lipo and mPEG/10%Agm_6-Lipo were not further investigated. Indeed, Anionic-Lipo does not interact with the cells, while mPEG/10%Agm_6-Lipo aggregates on the cell surface without cell internalization. Therefore, DH delivery was investigated by using 5%Agm_6-Lipo and mPEG/5%Agm_6-Lipo. Naked-Lipo and mPEG-Lipo were used as reference formulations.

3.3. Dexamethasone hemisuccinate-loaded liposomes

DH was loaded into the liposomes by remote loading prior to the surface modification with oligocations and mPEG. At pH 7.0, DH has LogD of −1.26 (Fig. SI-4A; Marvin software, version 19.27, by ChemAxon), which fits the recommended LogD values (from −1.5 to 1) for remote loading of amphipathic drugs into liposomes [57,58]. A preliminary study showed similar loading efficiency at pH 7.0 and 7.4 (Fig. SI-4B and C). Therefore, DH was loaded into liposomes at physiological pH of 7.4, which resulted in 9.1–11.3 wt/wt% DH loading capacity, corresponding to 36.2–44.9% loading efficiency.

Fig. 4A shows that the mPEG-DSPE post-insertion did not affect drug loading, but post-insertion of Agm_6-M-Oleate decreased DH loading capacity by ≈18%. These results suggest that post-insertion of mPEG does not alter the liposomal membrane permeability, whereas the oligocationic moieties induce bilayer leakiness, presumably due to repulsive charges on the liposome surface.

To investigate the effect of electrolytes and non-electrolytes on bilayer hydration, which in turn can impact on remote loading of drugs into liposomes [59,60], DH loading was also carried out in the presence of either the NaCl or dextrose under isosmotic conditions. The results (Fig. SI-5) did not show differences of drug loading among formulations, indicating that NaCl is a suitable excipient to obtain isotonic dispersions.

The results reported in Fig. 4B show that the DH-loaded liposomes have similar size, PDI, and zeta potential to DH-free liposomes described above. In particular, the similar zeta-potential of DH-free and DH-loaded liposomes suggests that DH does not interact with the liposome surface. Indeed, DH interaction with liposome surface would decrease the zeta potential of liposomes.

Cryo-transmission electron microscopy (Cryo-TEM) images of DH-loaded liposomes reported in Fig. 4C-F show the typical round-shaped morphology with the lipidic bilayers surrounding the inner aqueous compartment (images of drug-free liposomes are shown in Fig. SI-6). A negligible lamellarity due to the extrusion process [29] was observed in all formulations. All DH-loaded liposomes showed elongated structures corresponding to the Ca^{2+}/DH complex. A similar phenomenon was earlier reported with methylprednisolone hemisuccinate-loaded liposomes [61].

At pH 7.4, the size and zeta potential of DH-loaded Naked-Lipo and mPEG-Lipo were stable over 20 days, and negligible size increase and zeta potential decrease were observed in the case of 5%Agm_6-Lipo and mPEG/5%Agm_6-Lipo (Fig. SI-7) indicating that all formulations possess remarkable colloidal stability under this condition.

Large-angle light scattering (LALS) analyses by Apogee microflow cytometric system allowed for the evaluation of the colloidal stability of fluorescein-labeled DH-loaded liposomes in the vitreous. The instrument can distinguish the signals from the vitreal macromolecules and fluorescently labeled liposomes.

Fig. 5A shows the data of fluorescently labeled liposomes that were gated upon removal of the signals from the vitreal components.

Different LALS values at time 0 for the formulations indicate that they interact differently with the vitreous humor (Fig. 5B). In particular, 5%Agm_6-Lipo and mPEG/5%Agm_6-Lipo showed higher starting values than Naked-Lipo and mPEG-Lipo, suggesting that they underwent

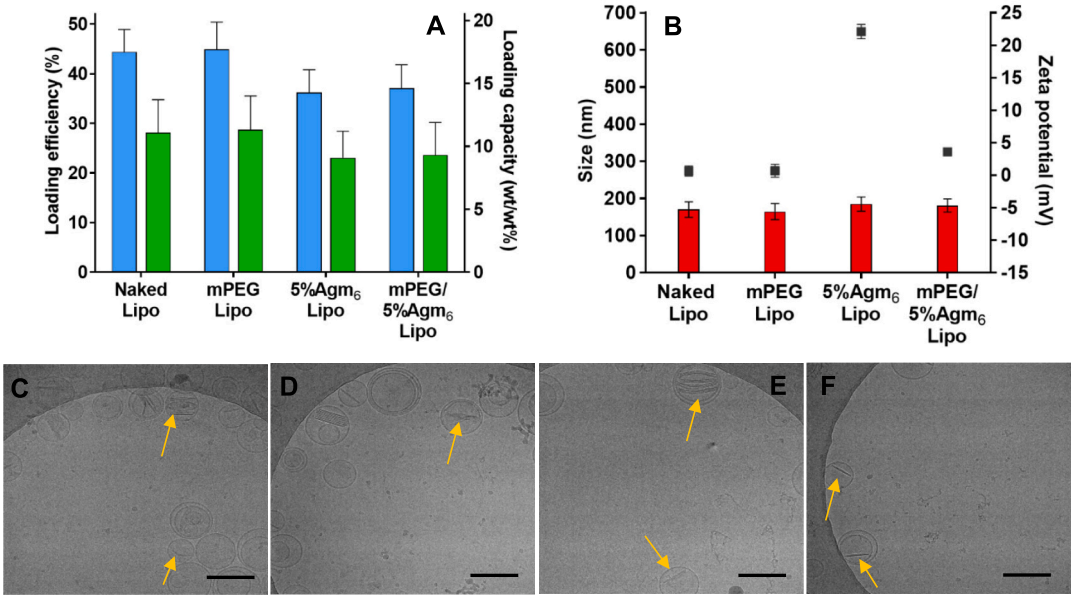

Fig. 4. A. DH loading efficiency (%, ■) and loading capacity (wt/wt%, ■) in liposomes. B. Size (■) and zeta-potential (■) profiles of DH-loaded liposome formulations with different coatings. Cryo-TEM images of the DH-loaded liposomes: Naked-Lipo (C), 5%Agm_6-Lipo (D), mPEG-Lipo (E), mPEG/5%Agm_6-Lipo (F); the samples were imaged at 57 K magnification. Yellow arrows indicate the nanocrystalline structures of Ca^{2+} dexamethasone hemisuccinate aggregates. Size bar: 200 nm. (For interpretation of the references to colour in this figure legend, the reader is referred to the web version of this article.)

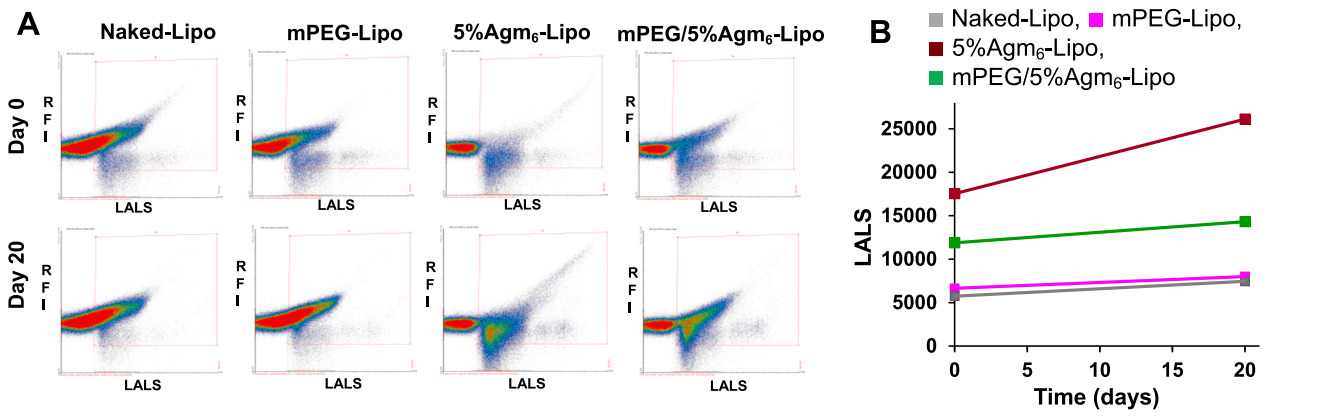

Fig. 5. Stability of DH-loaded liposomes in vitreous at 37 °C. A. Apogee flow cytometry profiles of liposomes. B. Correlation of the large angle light scattering signals *vs.* time of liposomes.

prompt dimensional changes in the vitreous. The LALS signals of Naked-Lipo and mPEG-Lipo did not increase over time, indicating that the size of these vesicles was stable in the vitreous. On the contrary, the LALS signal of 5%Agm_6-Lipo increased by about 50% in 20 days, indicating progressive aggregation of these liposomes in the vitreous. Notably, the increase of LALS signal was significantly reduced with mPEG-DSPE coating of 5%Agm_6-Lipo, showing remarkable PEG protection of the liposomes in the vitreous humor, which can also minimize the interference with vision upon administration.

Cytotoxicity of DH-loaded liposomes was assessed with ARPE-19 cells with increasing concentrations of DH up to 100 μM corresponding to 0.5 mg/mL liposome concentration.

The results reported in Fig. 6 show that DH-loaded liposomes were not cytotoxic over 6- and 24-h incubations. Free DH showed some cytotoxicity only at the highest drug concentration tested (100 μM) and 24 h exposure, which is in agreement with results reported in the literature [62].

The cytofluorimetric results reported in Fig. 7-i and SI-8 show that the DH-loaded liposomes behave similarly to their blank counterparts; cationic liposomes showed higher cell association than neutral ones. This confirms that the drug loading does not affect vesicle surfaces, and DH is not adsorbed on the liposome surface.

Confocal microscopy was used to study the internalization of the DH-loaded liposomes by the cultured ARPE19 cells. Figs. 7-ii A-B show that, similarly to DH-free liposomes (Figs. 3), the DH-loaded Naked-Lipo and mPEG-Lipo did not undergo cellular association or uptake. On the contrary, 5%Agm_6-Lipo and mPEG/5%Agm_6-Lipo showed remarkable cell association and disposition to the cytosol (Fig. 7-ii C—D). However, these formulations showed different patterns of cell association and entry. 5%Agm_6 formed large aggregates either on the cell surface or in the cytosol, while mPEG/5%Agm_6-Lipo accessed the cytosolic space generating small fluorescent spots similar to what was observed with the DH-free counterpart. Therefore, mPEG coating seems to reduce the clustering of cationic liposomes in the proximity of the cell membrane, thus facilitating cellular uptake.

3.4. *Dexamethasone hemisuccinate release*

Fig. 8 shows the *in vitro* release profiles of DH from liposomes at 37 °C in buffer at pH 7.4. All formulations displayed biphasic behavior with fast drug release within the first 24 h (Fig. SI-9), followed by a slow release for more than 30 days. This behavior can be explained by the equilibrium between non-complexed DH that can be promptly released and DH complexed with Ca^{2+} that is slowly released. The release profiles show that surface modification affects the DH release. 5%Agm_6-Lipo showed faster release compared to Naked-Lipo, suggesting that the post-insertion of the oligocationic-lipid moieties may affect the bilayer structure making it more permeable. This agrees with the slightly lower drug loading obtained after Agm_6-M-Oleate decoration (Fig. 4A). Both mPEG-Lipo and mPEG/5%Agm_6-Lipo showed lower levels of fast DH release and overall slower release than Naked-Lipo and 5%Arg_6-Lipo, which is in agreement with the previous observation that mPEG-DSPE

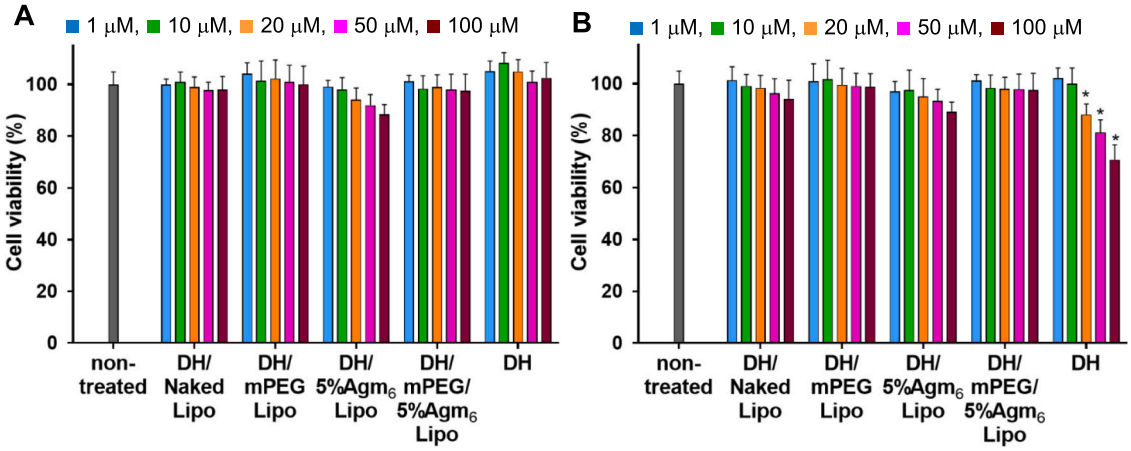

Fig. 6. Viability profile of ARPE-19 cells incubated with DH-loaded liposomes for 6 (A) and 24 h (B). Concentrations reported in legends refer to the DH or, in the case of drug-free liposomes, equimolar lipid concentration with respect to drug-loaded liposomes. Data are presented as mean ± SD ($n = 3$). Statistical analysis *versus* DH-loaded Nake-Lipo: * $p < 0.05$, ** $p < 0.01$, *** $p < 0.001$.

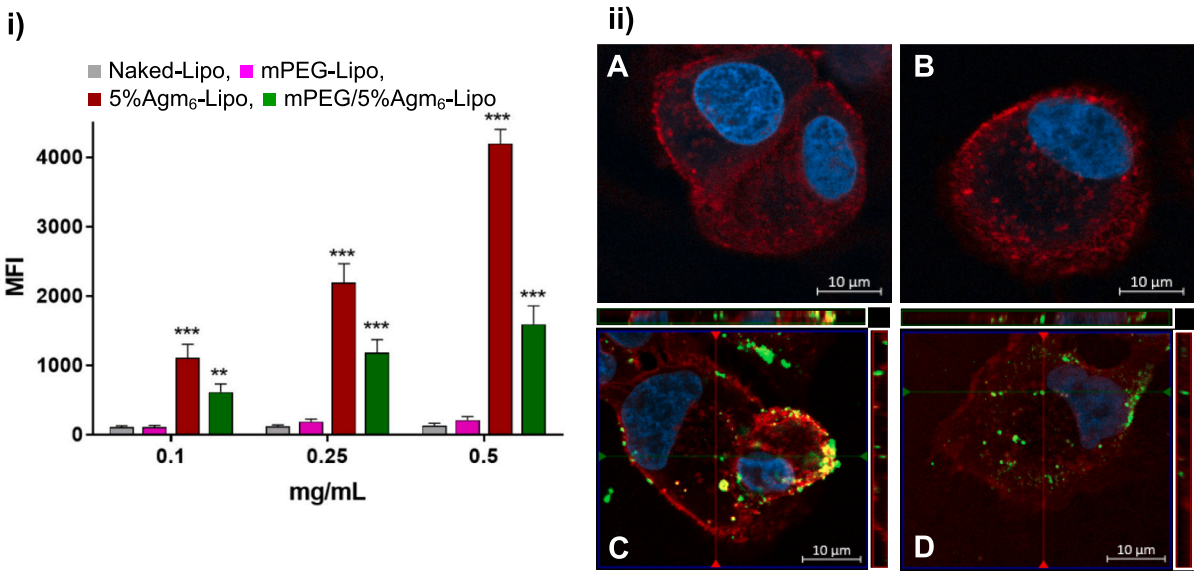

Fig. 7. i) Mean fluorescent intensity of ARPE-19 cells incubated with DH-loaded fluorescein-DHPE labeled liposomes at three liposome concentrations. Data are presented as Mean ± S.D. (n = 3). Statistical analysis was calculated *versus* DH-loaded Naked-Lipo. Ns: not significant, * $p < 0.05$, ** $p < 0.01$; *** $p < 0.001$, **** < 0.0001. ii) Confocal microscopic images of ARPE-19 cells incubated with DH-loaded Naked-Lipo (A), mPEG-Lipo (B), 5%Agm_6-Lipo (C), mPEG/5%Agm_6-Lipo (D). Panel C and D also include the *Z*-stack projections on the upper and right white frames. Nuclei of cells were stained in blue (DAPI), cell membranes in red (WGA-Alexa Fluor633), and liposomes in green (Fluorescein-DHPE). (For interpretation of the references to colour in this figure legend, the reader is referred to the web version of this article.)

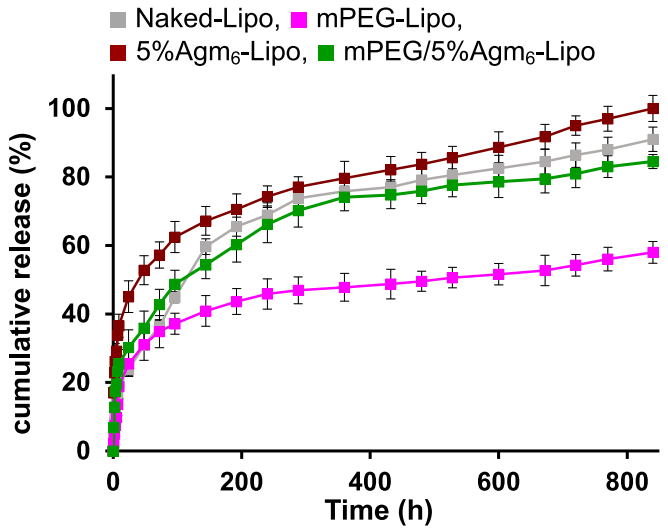

Fig. 8. DH release from liposomes. Data are presented as Mean ± S.D. ($n = 3$).

post-insertion may reduce the bilayer permeability of liposomes. In particular, mPEG-Lipo was found to yield a very slow DH release, suggesting that the polymer brush on the liposome surfaces increases the stability of the lipid bilayer and modulates the diffusivity of the drug across the lipid membrane [63].

3.5. Anti-inflammatory response

Strategies using glucocorticoids are frequently adopted in preclinical and clinical approaches [64–68], dexamethasone being the first-choice treatment providing neuroprotective effects by its anti-inflammatory activity [69]. Furthermore, dexamethasone has been shown to improve visual function in optic nerve traumatic injuries [70].

The anti-inflammatory activity of the DH-loaded liposomes was tested in ARPE-19 cells that were stimulated with lipopolysaccharide to activate the production of pro-inflammatory cytokines, such as IL-6, IL-8, IL-1β [71]. This endotoxin also stimulates retinal pigment epithelial cells to elicit an inflammatory response and pro-apoptotic signals. The cells respond to pro-inflammatory stimuli through several receptors, including CD14 and the toll-like receptors (TLRs), and regulate inflammatory signals in the retina [72]. In this study, the release of the pro-inflammatory marker IL-6 from ARPE-19 cells was monitored, and the anti-inflammatory activity of 1 and 10 μM DH was investigated. IL-6 was chosen as an inflammatory marker since its secretion by ARPE-19 cells upon pro-inflammatory challenge is largely prevailing other cytokines [73], and few studies demonstrated that IL-6 is a suitable marker to assess experimentally induced inflammation *in vitro* [74], oxidative stress [75] and the effect of anti-inflammatory drugs including dexamethasone [76] on ARPE-19 cells.

The results reported in Fig. 9 show that free DH and DH-loaded Naked-Lipo and mPEG-Lipo have low anti-inflammatory activity at 10 μM DH and none at 1 μM. Since little or no cell association or internalization was observed with Naked-Lipo and mPEG-Lipo (Fig. 7), the low anti-inflammatory activity was probably mediated by the DH released in the cell culture medium (Fig. 8). DH-loaded 5%Agm_6-Lipo and mPEG/5%Agm_6-Lipo remarkably decreased the inflammatory response. The reduction of IL-6 levels from non-treated control was 2.7 and 4.3 times with 1 μM DH-loaded 5%Agm_6-Lipo and mPEG/5%Agm_6-Lipo, respectively, and 3.9 and 9.4 times with 10 μM DH-loaded liposomes. The higher anti-inflammatory activity of 5%Agm_6-Lipo and mPEG/5%Agm_6-Lipo is in line with their efficient cell association and intracellular disposition in the ARPE19 cells (Fig. 7). The confocal data can explain the highest anti-inflammatory performance of mPEG/5%Agm_6-Lipo with respect to 5%Agm_6-Lipo. Indeed, while the latter associated more efficiently with cells but in large part remained on the liposome surface, the former possesses better access to the cell cytosol.

The low activity of free dexamethasone hemisuccinate reported in Fig. 9 is attributable to the short cell incubation time (1 h). Indeed, we previously found that 24 h cell incubation with dexamethasone hemisuccinate yielded significant anti-inflammatory activity, and this result was recently confirmed by similar studies reported in the literature [29,36]. However, it is worth to note that despite the short cell incubation, the 1 μM dexamethasone hemisuccinate equivalent mPEG/5%

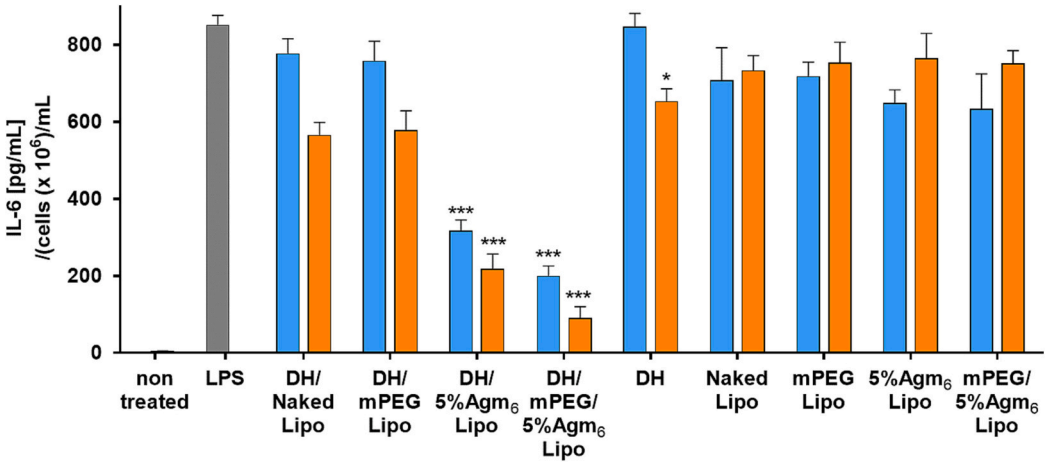

Fig. 9. IL-6 release by ARPE-19 cells after stimulation with LPS and treatment with liposomes. Cells were treated with DH-loaded liposomes at 1 μM (■) and 10 μM (■) drug concentration or equimolar concentration of drug-free liposomes. Untreated: cells that received neither LPS stimulation nor liposomes; LPS: cells stimulated only with LPS and did not receive liposomes. Data are presented as Mean ± S.D. ($n = 9$). $p > 0.05$, ns; * $p < 0.05$, ** $p < 0.01$; *** $p < 0.001$, **** < 0.0001 with the respective Naked-Lipo.

Agm_6 coated liposomes yielded about 76% anti-inflammatory activity, which is comparable to the effect obtained by 24 h TPH-1 cell incubation with free dexamethasone hemisuccinate reported in the literature.

3.6. Liposome distribution in ex vivo retinal layers and therapeutic effect

The drug-loaded liposomes were further studied in an *ex-vivo* retinal culture model for permeation and drug response (Fig. 10A). We used an air-medium interphase system, in which we placed the explanted retinae (together with the RPE) on top of the membrane, with the photoreceptor side facing the culture membrane. The liposomes were placed on the vitreal side of the retinal tissue, and permeation through all retinal layers was evaluated. The treatment with mPEG/5%Agm_6-Lipo resulted in a green fluorescent signal visible all through the tissue, including on the vitreal side, the inner plexiform layer (IPL), the inner nuclear layer (INL), the outer plexiform layer (OPL), the outer nuclear layer (ONL) and in the region of the outer segments (OS) contacting the RPE indicating that these liposomes diffused across the tissue (Fig. 10B). In the 5%Agm_6-Lipo treated tissue, also fluorescence -at a lower degree- was detected in the IPL, INL, and OPL. In addition, all groups showed fluorescence in the OS, which more likely corresponds to OS autofluorescence.

Under normal culture conditions, retinal cells suffer excessive stress and degenerate over time. Thus, *ex-vivo* retinas were treated with DH-loaded Naked-Lipo, mPEG-Lipo, 5%Agm_6-Lipo, and mPEG/5%Agm_6-Lipo to evaluate the efficiency of DH delivery by the liposomes to the target tissue. In addition, the TUNEL assay assessed cell death (Fig. 11A).

After 5 days of treatment with DH-loaded liposomes, retinas showed lower cell death (Fig. 11B), and higher thickness of the retina layers (Fig. 11C) compared to retinas treated with free DH, indicating that liposomes increased DH delivery, as well as neuroprotection. mPEG/5% Agm_6-Lipo was the most efficient formulation, with a surprisingly substantial reduction of cell death in the INL, which was also reflected in more cell rows in this layer.

4. Conclusions

The results reported in this study show that the combination of synthetic cell penetration enhancers (CPE) and mPEG can be successfully used to control the intravitreal behavior of colloidal drug delivery systems.

We have shown here that the combination of the Agm_6 and mPEG on

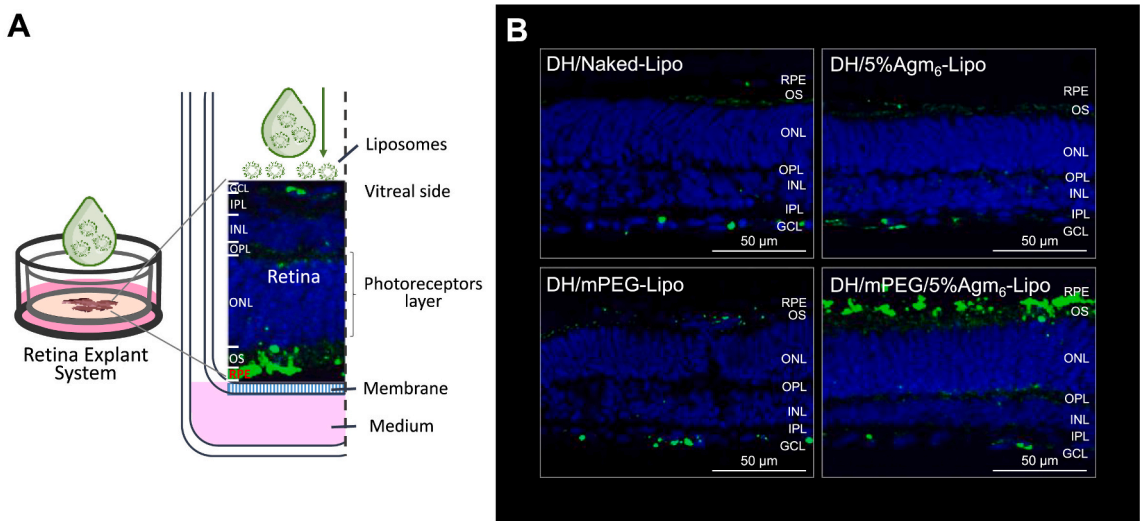

Fig. 10. DH loaded liposomes distribution in retinal explants sections. 14 μm sections were prepared from wild-type explanted retinae. (A) Diagram of the air-medium interphase system, in which explanted retinae faced the culture membrane on its photoreceptor side. Liposomes were added on the vitreal side of the retinae. (B) DH-loaded Naked-Lipo, mPEG-Lipo, 5%Agm_6-Lipo, and mPEG/5%Agm_6-Lipo-treated retinae. The treatment with mPEG/5%Agm_6-Lipo resulted in better penetration through all the retinal layers. Images were generated using 20× magnification. The scale bar is 50 μm. Abbreviations: GCL, ganglion cell layer; IPL, inner plexiform layer; INL, Inner nuclear layer; OPL, outer plexiform layer; ONL, Outer nuclear layer; OS, outer segments; RPE: Retinal Pigmented Epithelium.

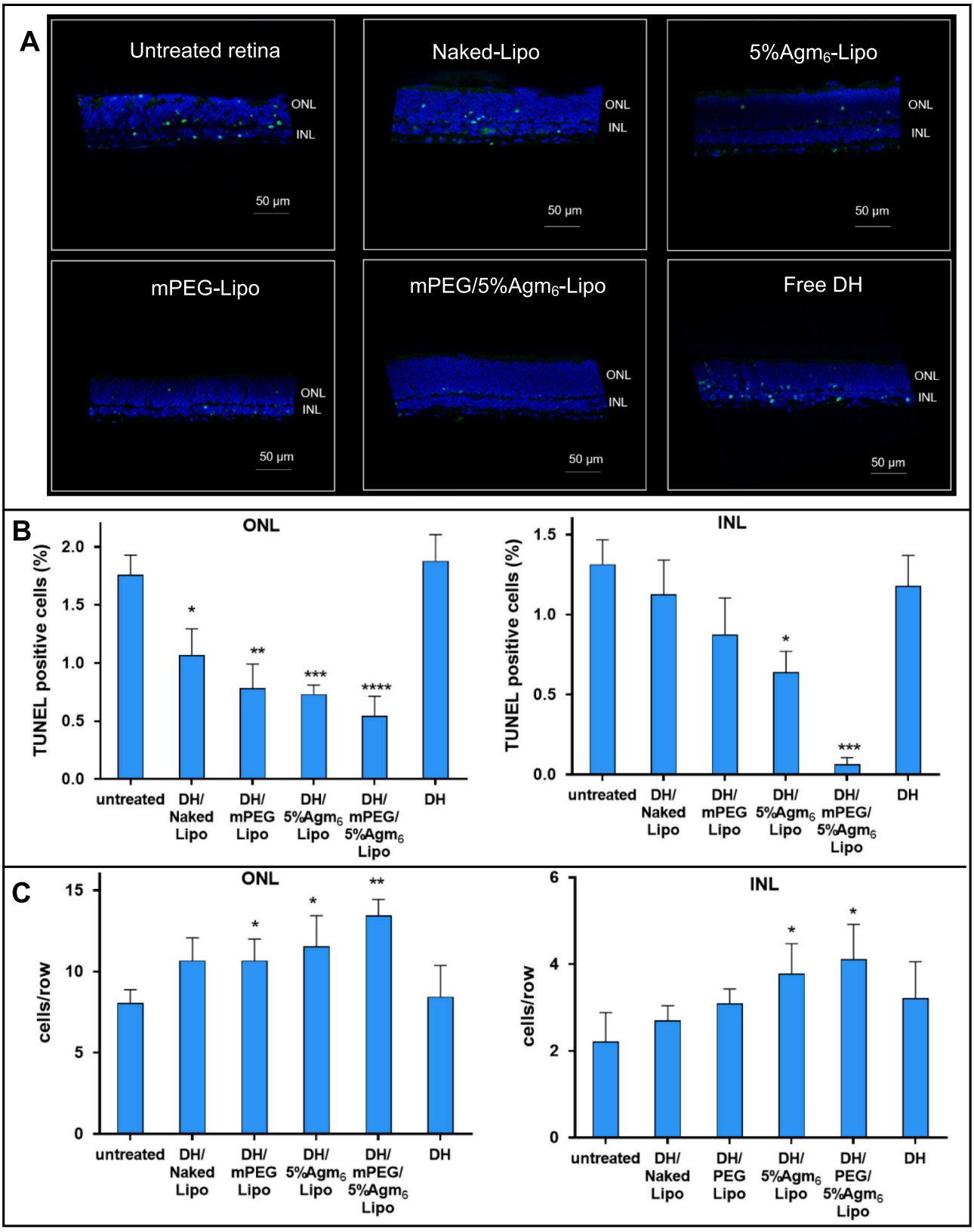

Fig. 11. A. Microscopic analysis of retinal explant sections by TUNEL assay. Sections of wild-type mice explanted retinas treated with DH-loaded liposomes were imaged after treatment. TUNEL-positive cells (green) and the DAPI-stained nuclei (blue) were quantified. Images are taken with 20× magnification. Scale bar 50 µm. B. Graphical representation of TUNEL-positive cells and C. cell rows count in ONL and INL of different treatment groups. Data are presented as Mean ± SD ($N = 3$ retinas). Statistical analysis was performed *versus* untreated retina. ns: not significant, *$p < 0.05$; ** $p < 0.01$; *** $p < 0.001$, ****$p < 0.0001$. (For interpretation of the references to colour in this figure legend, the reader is referred to the web version of this article.)

the liposome surface offers the opportunity to tailor the diffusivity of the liposomes in the vitreous, allowing docking to the retina upon intravitreal treatment. The coating of Agm_6 decorated liposomes with mPEG provides an effective therapeutic anti-inflammatory outcome *in vitro and ex-vivo*, resulting from a combination of factors, including high intracellular drug delivery and low carrier cytotoxicity. On the other hand, further investigations are required to elucidate the effect of mPEG and Agm_6 on the mechanism regulating the liposome/cell membrane interaction, endocytosis, and intracellular trafficking.

CRediT authorship contribution statement

M.D. Al-Amin: Methodology, Investigation, Data curation, Writing – original draft. **Francesca Mastrotto:** Methodology, Validation, Writing – review & editing. **Astrid Subrizi:** Methodology, Validation, Writing – review & editing. **Merve Sen:** Formal analysis, Data curation, Methodology. **Tiina Turunen:** Investigation, Data curation. **Blanca Arango-Gonzalez:** Supervision, Visualization, Writing – review & editing. **Marius Ueffing:** Supervision, Visualization, Writing – review & editing. **Alessio Malfanti:** Methodology, Writing – original draft. **Arto Urtti:** Supervision, Visualization, Writing – review & editing. **Stefano Salmaso:** Conceptualization, Supervision, Investigation, Funding acquisition, Project administration, Writing – review & editing, Writing – original draft. **Paolo Caliceti:** Formal analysis, Visualization, Funding acquisition, Writing – review & editing.

Data availability

Data will be made available on request.

Acknowledgments

This project has received funding from the European Union's Horizon 2020 research and innovation program under the Marie Skłodowska-Curie grant agreement N° 722717, and was supported by FFB (Grant PPA-0717-0719-RAD), the Kerstan Foundation, and the ProRetina Foundation.

Appendix A. Supplementary data

Supplementary data to this article can be found online at https://doi.org/10.1016/j.jconrel.2023.01.027.

References

[1] W.L. Wong, X. Su, X. Li, C.M.G. Cheung, R. Klein, C.-Y. Cheng, T.Y. Wong, Global prevalence of age-related macular degeneration and disease burden projection for 2020 and 2040: a systematic review and meta-analysis, The Lancet Glob. Health 2 (2014) e106–e116.
[2] D. Wakefield, A. Lloyd, The role of cytokines in the pathogenesis of inflammatory eye disease, Cytokine 4 (1992) 1–5.
[3] S. Cornel, I.D. Adriana, T.C. Mihaela, S. Speranta, D.S. Algerino, B. Mehdi, H.-R. Jalaladin, Anti-vascular endothelial growth factor indications in ocular disease, Roman. J. Ophthalmol. 59 (2015) 235–242.
[4] E.M. Del Amo, A.K. Rimpelä, E. Heikkinen, O.K. Kari, E. Ramsay, T. Lajunen, M. Schmitt, L. Pelkonen, M. Bhattacharya, D. Richardson, A. Subrizi, T. Turunen, M. Reinisalo, J. Itkonen, E. Toropainen, M. Casteleijn, H. Kidron, M. Antopolsky, K. S. Vellonen, M. Ruponen, A. Urtti, Pharmacokinetic aspects of retinal drug delivery, Prog. Retin. Eye Res. 57 (2017) 134–185.
[5] R.D. Jager, L.P. Aiello, S.C. Patel, E.T. Cunningham Jr., Risks of Intravitreous Injection: A Comprehensive Review, (Philadelphia, Pa.) 24, 2004, pp. 676–698.
[6] E.J. Campos, A. Campos, J. Martins, A.F. Ambrósio, Opening eyes to nanomedicine: where we are, challenges and expectations on nanotherapy for diabetic retinopathy, Nanomedicine 13 (2017) 2101–2113.
[7] M.A. Kamaleddin, Nano-ophthalmology: applications and considerations, Nanomedicine 13 (2017) 1459–1472.
[8] U.B. Kompella, A.C. Amrite, R. Pacha Ravi, S.A. Durazo, Nanomedicines for back of the eye drug delivery, gene delivery, and imaging, Prog. Retin. Eye Res. 36 (2013) 172–198.
[9] L. Kou, Y.D. Bhutia, Q. Yao, Z. He, J. Sun, V. Ganapathy, Transporter-guided delivery of nanoparticles to improve drug permeation across cellular barriers and drug exposure to selective cell types, Front. Pharmacol. 9 (2018) 27.
[10] A. Sepahvandi, M. Eskandari, F.J.B. Moztarzadeh, Drug Delivery Systems to the Posterior Segment of the Eye: Implants and Nanoparticles 6, 2016, pp. 276–283.
[11] I.P. Kaur, S. Kakkar, Nanotherapy for posterior eye diseases, J. Control. Release 193 (2014) 100–112.
[12] R. Zhang, J. Qian, X. Li, Y. Yuan, Treatment of experimental autoimmune uveoretinitis with intravitreal injection of infliximab encapsulated in liposomes, Br. J. Ophthalmol. 101 (2017) 1731–1738.
[13] A. Bochot, E. Fattal, Liposomes for intravitreal drug delivery: a state of the art, J. Control. Release 161 (2012) 628–634.
[14] J.R. Villanueva, L.R. Villanueva, M.G. Navarro, Pharmaceutical technology can turn a traditional drug, dexamethasone into a first-line ocular medicine. A global perspective and future trends, Int. J. Pharm. 516 (2017) 342–351.
[15] M. Honda, T. Asai, N. Oku, Y. Araki, M. Tanaka, N. Ebihara, Liposomes and nanotechnology in drug development: focus on ocular targets, Int. J. Nanomedicine 8 (2013) 495.
[16] I. Melgar-Asensio, I. Kandela, F. Aird, S.R. Darjatmoko, C. de Los Rios, C. M. Sorenson, D.M. Albert, N. Sheibani, J. Henkin, Extended intravitreal rabbit eye residence of nanoparticles conjugated with cationic arginine peptides for intraocular drug delivery: in vivo imaging, Invest. Ophthalmol. Vis. Sci. 59 (2018) 4071–4081.
[17] M. Bhattacharya, S. Sarkhel, J. Peltoniemi, R. Broadbridge, M. Tuomainen, S. Auriola, A. Urtti, Differentially cleaving peptides as a strategy for controlled drug release in human retinal pigment epithelial cells, J. Control. Release 251 (2017) 37–48.
[18] L.N. Johnson, S.M. Cashman, S.P. Read, R. Kumar-Singh, Cell penetrating peptide POD mediates delivery of recombinant proteins to retina, cornea and skin, Vis. Res. 50 (2010) 686–697.
[19] V. Chaudhary, J. Barbosa, W.C. Lam, M. Mak, E. Mavrikakis, P.S. Mohaghegh, Ozurdex in age-related macular degeneration as adjunct to ranibizumab (the OARA study), Canadian journal of ophthalmology, J. Canadien d'Ophtalmol. 51 (2016) 302–305.
[20] D. Röck, K.U. Bartz-Schmidt, T. Röck, Risk factors for and management of anterior chamber intravitreal dexamethasone implant migration, BMC Ophthalmol. 19 (2019) 1–7.
[21] A. Sadeghi, M. Ruponen, J. Puranen, S. Cao, R. Ridolfo, S. Tavakoli, E. Toropainen, T. Lajunen, V.P. Ranta, J. van Hest, A. Urtti, Imaging, quantitation and kinetic modelling of intravitreal nanomaterials, Int. J. Pharm. 621 (2022), 121800.
[22] S. Lei, W.-C. Lam, Efficacy and safety of dexamethasone intravitreal implant for refractory macular edema in children, Can. J. Ophthalmol. 50 (2015) 236–241.
[23] A. Malfanti, F. Mastrotto, Y. Han, P. Král, A. Balasso, A. Scomparin, S. Pozzi, R. Satchi-Fainaro, S. Salmaso, P. Caliceti, Novel oligo-Guanidyl-PEG carrier forming rod-shaped Polyplexes, Mol. Pharm. 16 (2019) 1678–1693.
[24] S. Sakaguchi, A new color reaction of protein and arginine, J. Biochem. 5 (1925) 25–31.
[25] A. Bangham, M.M. Standish, J.C. Watkins, Diffusion of univalent ions across the lamellae of swollen phospholipids, J. Mol. Biol. 13 (1965), 238-252.
[26] M.C. Goldschmidt, B.M. Lockhart, Simplified rapid procedure for determination of agmatine and other guanidino-containing compounds, Anal. Chem. 43 (1971) 1475–1479.
[27] J.C.M. Stewart, Colorimetric determination of phospholipids with ammonium ferrothiocyanate, Anal. Biochem. 104 (1980) 10–14.
[28] G.E.C. Sims, T.J. Snape, A method for the estimation of polyethylene glycol in plasma protein fractions, Anal. Biochem. 107 (1980) 60–63.
[29] M.D. Al-Amin, F. Bellato, F. Mastrotto, M. Garofalo, A. Malfanti, S. Salmaso, P. Caliceti, Dexamethasone loaded liposomes by thin-film hydration and microfluidic procedures: formulation challenges, Int. J. Mol. Sci. 21 (2020) 1611–1632.
[30] A. Balasso, A. Subrizi, S. Salmaso, F. Mastrotto, M. Garofalo, M. Tang, M. Chen, H. Xu, A. Urtti, P. Caliceti, Screening of chemical linkers for development of pullulan bioconjugates for intravitreal ocular applications, Eur. J. Pharm. Sci. 161 (2021), 105785.
[31] Q. Xu, N.J. Boylan, J.S. Suk, Y.-Y. Wang, E.A. Nance, J.-C. Yang, P.J. McDonnell, R. A. Cone, E.J. Duh, J. Hanes, Nanoparticle diffusion in, and microrheology of, the bovine vitreous ex vivo, J. Control. Release 167 (2013) 76–84.
[32] B. Arango-Gonzalez, A. Szabo, G. Pinzon-Duarte, A. Lukats, E. Guenther, K. Kohler, In vivo and in vitro development of S- and M-cones in rat retina, Invest. Ophthalmol. Vis. Sci. 51 (2010) 5320–5327.
[33] Y. Zhu, B. Cao, A. Tolone, J. Yan, G. Christensen, B. Arango-Gonzalez, M. Ueffing, F. Paquet-Durand, In vitro model Systems for Studies into Retinal Neuroprotection, Front. Neurosci. 16 (2022) 1–15.
[34] B. Arango-Gonzalez, M. Sen, R. Guarascio, K. Ziaka, E.M. del Amo, K. Hau, H. Poultney, R. Asfahani, A. Urtti, T.-F. Chou, S. Bolz, R.J. Deshaies, W. Haq, M. E. Cheetham, M. Ueffing, Inhibition of VCP preserves retinal structure and function in autosomal dominant retinal degeneration, bioRxiv 2020 (2020) 1–42.
[35] Y. Avnir, K. Turjeman, D. Tulchinsky, A. Sigal, P. Kizelsztein, D. Tzemach, A. Gabizon, Y. Barenholz, Fabrication principles and their contribution to the superior in vivo therapeutic efficacy of nano-liposomes remote loaded with glucocorticoids, PLoS One 6 (2011), e25721.
[36] N.V. Dubashynskaya, A.N. Bokatyi, A.S. Golovkin, I.V. Kudryavtsev, M. K. Serebryakova, A.S. Trulioff, Y.A. Dubrovskii, Y.A. Skorik, Synthesis and characterization of novel succinyl chitosan-dexamethasone conjugates for potential intravitreal dexamethasone delivery, Int. J. Mol. Sci. 22 (2021) 10960.
[37] G. Christensen, L. Barut, D. Urimi, N. Schipper, F. Paquet-Durand, Investigating ex vivo animal models to test the performance of Intravitreal liposomal drug delivery systems, Pharmaceutics 13 (2021) 1013.

[38] M. Mashal, N. Attia, G. Puras, G. Martínez-Navarrete, E. Fernández, J.L. Pedraz, Retinal gene delivery enhancement by lycopene incorporation into cationic niosomes based on DOTMA and polysorbate 60, J. Control. Release 254 (2017) 55–64.
[39] E. Ramsay, M. Raviña, S. Sarkhel, S. Hehir, N.R. Cameron, T. Ilmarinen, H. Skottman, J. Kjems, A. Urtti, M. Ruponen, Avoiding the pitfalls of siRNA delivery to the retinal pigment epithelium with physiologically relevant cell models, Pharmaceutics 12 (2020) 667.
[40] S. Bersani, S. Salmaso, F. Mastrotto, E. Ravazzolo, A. Semenzato, P. Caliceti, Star-like oligo-arginyl-maltotriosyl derivatives as novel cell-penetrating enhancers for the intracellular delivery of colloidal therapeutic systems, Bioconjug. Chem. 23 (2012) 1415–1425.
[41] B.S. Schuster, J.S. Suk, G.F. Woodworth, J. Hanes, Nanoparticle diffusion in respiratory mucus from humans without lung disease, Biomaterials 34 (2013) 3439–3446.
[42] K. Maisel, M. Reddy, Q. Xu, S. Chattopadhyay, R. Cone, L.M. Ensign, J. Hanes, Nanoparticles coated with high molecular weight PEG penetrate mucus and provide uniform vaginal and colorectal distribution in vivo, Nanomedicine 11 (2016) 1337–1343.
[43] A. Lechanteur, T. Furst, B. Evrard, P. Delvenne, P. Hubert, G. Piel, PEGylation of lipoplexes: the right balance between cytotoxicity and siRNA effectiveness, Eur. J. Pharm. Sci. 93 (2016) 493–503.
[44] S. Tavakoli, O.K. Kari, T. Turunen, T. Lajunen, M. Schmitt, J. Lehtinen, F. Tasaka, P. Parkkila, J. Ndika, T. Viitala, Diffusion and protein corona formation of lipid-based nanoparticles in the vitreous humor: profiling and pharmacokinetic considerations, Mol. Pharm. 18 (2020) 699–713.
[45] K. Romøren, B.J. Thu, N.C. Bols, Ø. Evensen, Transfection efficiency and cytotoxicity of cationic liposomes in salmonid cell lines of hepatocyte and macrophage origin, Biochim. Biophys. Acta (BBA)-Biomembranes 1663 (2004) 127–134.
[46] S. Takano, Y. Aramaki, S. Tsuchiya, Physicochemical properties of liposomes affecting apoptosis induced by cationic liposomes in macrophages, Pharm. Res. 20 (2003) 962–968.
[47] A. Malfanti, A. Scomparin, S. Pozzi, H. Gibori, A. Krivitsky, R. Blau, R. Satchi-Fainaro, F. Mastrotto, P. Caliceti, S. Salmaso, Oligo-guanidyl targeted bioconjugates forming rod shaped polyplexes as a new nanoplatform for oligonucleotide delivery, J. Control. Release 310 (2019) 58–73.
[48] M. Barattin, A. Mattarei, A. Balasso, C. Paradisi, L. Cantù, E. Del Favero, T. Viitala, F. Mastrotto, P. Caliceti, S. Salmaso, pH-controlled liposomes for enhanced cell penetration in tumor environment, ACS Appl. Mater. Interfaces 10 (2018) 17646–17661.
[49] X. Wei, R. Cohen, Y. Barenholz, Insights into composition/structure/function relationships of Doxil® gained from "high-sensitivity" differential scanning calorimetry, Eur. J. Pharm. Biopharm. 104 (2016) 260–270.
[50] M. Roursgaard, K.B. Knudsen, H. Northeved, M. Persson, T. Christensen, P.E. K. Kumar, A. Permin, T.L. Andresen, T. Gjetting, J. Lykkesfeldt, In vitro toxicity of cationic micelles and liposomes in cultured human hepatocyte (HepG2) and lung epithelial (A549) cell lines, Toxicol. in Vitro 36 (2016) 164–171.
[51] S. Tavakoli, O.K. Kari, T. Turunen, T. Lajunen, M. Schmitt, J. Lehtinen, F. Tasaka, P. Parkkila, J. Ndika, T. Viitala, H. Alenius, A. Urtti, A. Subrizi, Diffusion and protein Corona formation of lipid-based nanoparticles in the vitreous humor: profiling and pharmacokinetic considerations, Mol. Pharm. 18 (2021) 699–713.
[52] L. Pitkänen, M. Ruponen, J. Nieminen, A. Urtti, Vitreous is a barrier in nonviral gene transfer by cationic lipids and polymers, Pharm. Res. 20 (2003) 576–583.
[53] S. Salmaso, P. Caliceti, Self assembling nanocomposites for protein delivery: supramolecular interactions of soluble polymers with protein drugs, Int. J. Pharm. 440 (2013) 111–123.
[54] C.R. Miller, B. Bondurant, S.D. McLean, K.A. McGovern, D.F. O'Brien, Liposome–cell interactions in vitro: effect of liposome surface charge on the binding and endocytosis of conventional and sterically stabilized liposomes, Biochemistry 37 (1998) 12875–12883.
[55] D.J. Chin, R.M. Straubinger, S. Acton, I. Näthke, F.M. Brodsky, 100-kDa polypeptides in peripheral clathrin-coated vesicles are required for receptor-mediated endocytosis, Proc. Natl. Acad. Sci. U. S. A. 86 (1989) 9289–9293.
[56] V.M. Steffes, Z. Zhang, S. MacDonald, J. Crowe, K.K. Ewert, B. Carragher, C. S. Potter, C.R. Safinya, PEGylation of paclitaxel-loaded cationic liposomes drives steric stabilization of bicelles and vesicles thereby enhancing delivery and cytotoxicity to human cancer cells, ACS Appl. Mater. Interfaces 12 (2019) 151–162.
[57] D. Zucker, D. Marcus, Y. Barenholz, A. Goldblum, Liposome drugs' loading efficiency: a working model based on loading conditions and drug's physicochemical properties, J. Control. Release 139 (2009) 73–80.
[58] Y. Barenholz, Y. Naparstek, Y. Avnir, R. Ulmansky, Use of Liposomal Glucocorticoids for Treating Inflammatory States, in, Google Patents, 2010.
[59] A. Roy, R. Dutta, N. Kundu, D. Banik, N. Sarkar, A comparative study of the influence of sugars sucrose, Trehalose, and maltose on the hydration and diffusion of DMPC lipid bilayer at complete hydration: investigation of structural and spectroscopic aspect of lipid–sugar interaction, Langmuir 32 (2016) 5124–5134.
[60] C.S. Pereira, P.H. Hünenberger, Interaction of the sugars trehalose, maltose and glucose with a phospholipid bilayer: a comparative molecular dynamics study, J. Phys. Chem. B 110 (2006) 15572–15581.
[61] Y. Avnir, R. Ulmansky, V. Wasserman, S. Even-Chen, M. Broyer, Y. Barenholz, Y. Naparstek, Amphipathic weak acid glucocorticoid prodrugs remote-loaded into sterically stabilized nanoliposomes evaluated in arthritic rats and in a beagle dog: a novel approach to treating autoimmune arthritis, Arthritis Rheum. 58 (2008) 119–129.
[62] C.K. Yeung, K.P. Chan, C.K. Chan, C.P. Pang, D.S. Lam, Cytotoxicity of triamcinolone on cultured human retinal pigment epithelial cells: comparison with dexamethasone and hydrocortisone, Jpn. J. Ophthalmol. 48 (2004) 236–242.
[63] H. Wang, P. Zhao, W. Su, S. Wang, Z. Liao, R. Niu, J. Chang, PLGA/polymeric liposome for targeted drug and gene co-delivery, Biomaterials 31 (2010) 8741–8748.
[64] C.C. Wykoff, Impact of intravitreal pharmacotherapies including antivascular endothelial growth factor and corticosteroid agents on diabetic retinopathy, Curr. Opin. Ophthalmol. 28 (2017) 213–218.
[65] A. Capone Jr., M.A. Singer, D.G. Dodwell, R.F. Dreyer, K.T. Oh, D.B. Roth, J. G. Walt, L.C. Scott, D.A. Hollander, Efficacy and safety of two or more dexamethasone intravitreal implant injections for treatment of macular edema related to retinal vein occlusion (Shasta study), Retina 34 (2014) 342–351.
[66] E. Kickova, A. Sadeghi, J. Puranen, S. Tavakoli, M. Sen, V.P. Ranta, B. Arango-Gonzalez, S. Bolz, M. Ueffing, S. Salmaso, P. Caliceti, E. Toropainen, M. Ruponen, A. Urtti, Pharmacokinetics of pullulan-dexamethasone conjugates in retinal drug delivery, Pharmaceutics 14 (2021).
[67] O. Ayar, A. Alpay, Y. Koban, M.O. Akdemir, S. Yazgan, S. Canturk Ugurbas, S. H. Ugurbas, The effect of dexamethasone intravitreal implant on retinal nerve fiber layer in patients diagnosed with branch retinal vein occlusion, Curr. Eye Res. 42 (2017) 1287–1292.
[68] H. Zygmunt, K. Raczyńska, W. Czuszyński, Idiopathic, bilateral panuveitis–efficacy of general steroidotherapy and intravitreal dexamethason injection. Case report, Klin. Ocz. 114 (2012) 44–49.
[69] I.M. Ábrahám, P. Meerlo, P.G.M. Luiten, Concentration dependent actions of glucocorticoids on neuronal viability and survival, Dose-Response 4 (2006) dose-response.
[70] T. Chan, J. Wong, R. Ram, S. Amrith, Visual recovery following treatment with very high dose corticosteroid in traumatic optic neuropathy, Singap. Med. J. 37 (1996) 216–217.
[71] K.W. Leung, C.J. Barnstable, J. Tombran-Tink, Bacterial endotoxin activates retinal pigment epithelial cells and induces their degeneration through IL-6 and IL-8 autocrine signaling, Mol. Immunol. 46 (2009) 1374–1386.
[72] K. Mai, J.J.Y. Chui, N. Di Girolamo, P.J. McCluskey, D. Wakefield, Role of toll-like receptors in human iris pigment epithelial cells and their response to pathogen-associated molecular patterns, J. Inflamm. 11 (2014) 1–12.
[73] F. Duan, W. Zeng, Y. Zhang, D. Li, K. Wu, Lipopolysaccharide enhances HSV-1 replication and inflammatory factor release in the ARPE-19 cells, Heliyon 8 (2022), e11787.
[74] A. Bernardo-Colón, M. Lerner, S.P. Becerra, Pigment epithelium-derived factor is an interleukin-6 antagonist in the RPE: insight of structure-function relationships, Front. Physiol. 2420 (2022) 1–9.
[75] A. Subrizi, E. Toropainen, E. Ramsay, A.J. Airaksinen, K. Kaarniranta, A. Urtti, Oxidative stress protection by exogenous delivery of rhHsp70 chaperone to the retinal pigment epithelium (RPE), a possible therapeutic strategy against RPE degeneration, Pharm. Res. 32 (2015) 211–221.
[76] V. Tambe, N. Raval, P. Gondaliya, P. Bhattacharya, K. Kalia, R.K. Tekade, To investigate fit-to-purpose nanocarrier for non-invasive drug delivery to posterior segment of eye, J. Drug Deliv. Sci. Technol. 61 (2021), 102222.